J. Bangladesh Acad. Sci. 50(1); 71-98: March 2026 DOI:https://doi.org/10.3329/jbas.v50i1.85275

Journal of Bangladesh Academy of Sciences

Journal homepage: http://www.bas.org.bd/publications/jbas.html

Research Article

A deterministic and fractional order mathematical approach: Prey-predator dynamics in higher education systems

Md. Asraful Islam* and Tanvir Ahmed

Department of Mathematics, Jagannath University, Dhaka, Bangladesh

ARTICLE INFO

Article History

Received: 27 October 2025
Revised: 01 Februray 2026
Accepted: 08 February 2026

Keywords: Academic stress, Under-graduate students, Graduate students, Fractional order, Lyapunov exponent, Bifurcation.

ABSTRACT

This study explores the dynamic relationship between academic stress and student populations in higher education using a deterministic and fractional-order prey-predator framework, where stress acts as the predator and students as the prey. Equilibrium conditions are used to study the system's stability, while bifurcation analyses reveals critical transitions, including flip, fold, Hopf, and Neimark-Sacker bifurcations. Global stability analysis provides insight into the long-term behavior of students under academic constraints, and criteria for persistence and the basic reproduction number are established. The fractional-order approach effectively captures memory effects that influence students' responses. Lyapunov exponents and numerical simulations further elucidate stability thresholds and the emergence of chaotic dynamics. Additionally, bifurcation diagram and basin of attraction analyses illustrate shifts in equilibrium states. The findings suggest that policy interventions targeting highly sensitive factors can significantly influence system dynamics, leadingto measurable changes in academic stress levels and overall stability. The study provides both theoretical and practical insights, demonstrating that undergraduate students tend to experience higher levels of stress than graduate students, primarily due to strict curriculum, more frequent examinations, and limited autonomy in undergraduate education.

Introduction

Early in the 20th century, Alfred Lotka and Vito Volterra independently developed the prey-predator model; the historical foundation of this model is the early application of mathematics to biological and ecological processes. Lotka (1925) derived these equations for the study of chemical processes,and later for biological systems.Volterra(1926) used a similar approach for the research of fish dynamics in the Adriatic Sea. Currently referred to as the Lotka-Volterra equations, they describe interactions between two populations: herbivores and predators, and carnivores. It holds that their interaction controls population dynamics: without predators, prey expand exponentially, and predator populations decline. Since ecosystems, epidemiology, and economics are more dynamic systems, this model has been extended to include those disciplines. This model has been extended to include ecologies, epidemiology, and economics since these are more dynamic systems. A deterministic predator-prey model (Amri et al., 2023; Wang and Yang, 2025) to investigate the effects of velocity on ant predator behavior, refuge dynamics, and interactions. It has performed the stability analysis and found that, at critical predator death rates, the predator-free equilibrium, coexistence conditions, and transcritical bifurcations are globally asymptotically stable.

*Corresponding author: <asraful@math.jnu.ac.bd>

Using a pest management model (Yu et al., 2019) with state feedback control and optimization helps one to control pest numbers. A predator–prey model (Ska et al., 2021; Ahmed et al., 2025) with fear, refuge, and additional food exhibits stability, oscillations, and chaotic dynamics. It has investigated an eco-epidemiological model (Sha et al., 2019) in which the growth of prey and disease transmission is suppressed by fear induced by predators. With conditions for local stability developed, this yields backward bifurcation, instability, oscillations, and chaotic dynamics.

The mechanisms by which fear, shelter, and hunting cooperation influence the dynamics between predators and prey (Mondal et al., 2022) have been extensivelyinvestigated. Establishing global dynamical behavior requirements, initially, they analyze a stochastic two-predator one-prey model with Lévy noise and distributed delays (Tuerxun et al., 2020). It has investigated a nonautonomous predator-prey system (Bai et al., 2020) with a Beddington-DeAngelis response and built appropriate criteria for the global asymptotic stability of boundary solutions. A two-parameter discrete predator-prey model is addressed by Hone et al. (2010). This model sets criteria for stability and bifurcation dynamics and expands Murray's framework. The stability, permanence, extinction, and ecological effects of a stochastic four-species predator-prey model with disease (Gokila et al., 2023) are investigated via simulations. Using geometric methods, a general predator–prey model (Zhu et al., 2022) with state-dependent impulses is examined to determine the conditions for the existence of order-1 periodic solutions and their stability. With specific attention on the function it performs in the creation of patterns, a study is conducted on the effect of prey refuge on the dynamics of predators and prey using bifurcation theory and numerical simulations.

Rising and declining numbers of prey and predators, respectively, reflect the phases of mutual benefit and predator suppression as refuge depths broaden. It analyzed the effects of prey refuges on predator-prey dynamics, considering both constant-proportional and fixed-number refuges. The results (Ma et al., 2009) reveal that, aside from some destabilizing circumstances, prey refuges increase prey density, reduce predator density and usually stabilize the equilibrium. They investigated stability and Hopf bifurcation dynamics in a stage-structured predator-prey model (Bai and Li, 2019) with extra predator food and prey refuge. It studies a predator-prey model including both discrete and distributed delays; the discrete delay is considered as a bifurcation parameter. Hopf bifurcation occurs at a turning point (Ma et al., 2009; Misra and Dubey, 2010), and normal form theory defines the stability and features of periodic solutions.

The dynamics of an impulsive state feedback-controlled Holling type II predator-prey system (Jiang et al., 2007) is investigated theoretically and numerically. Lyapunov exponents and bifurcation analysis help identify periodic and chaotic behavior, thereby demonstrating the effectiveness of the control approach. Using a Markovian switching technique to address telephone noise modeling, a stochastic regime-switching predator-prey model (Liu et al., 2018) is built with harvesting and distributed delays. It explores extinction scenarios, population persistence, and ideal harvesting strategies in detail. Analysis of a non-autonomous ratio-dependent predator-prey system (Bai et al., 2014) driven by Lévy noise reveals global positive solutions, stochastic boundedness, persistence, extinction conditions, and asymptotic behavior. Numerical simulations help verify these results. Stability and bifurcation analysis (Hu and Cao, 2017) of a nonlinear Michaelis-Menten type predator harvesting system are investigated. Equilibrium existence and stability are found using numerical and mathematical methods. Moreover, numerical simulations investigate the Bogdanov-Takens bifurcation under a universal unfolding around the cusp, therefore verifying the theoretical conclusions. The worldwide attraction and permanency criteria of

a stage-structured predator-prey model (Song et al., 2009) are investigated in this work.

An examination of stability, Hopf bifurcation occurrence, bifurcation direction, and periodic solution stability is conducted through theoretical analysis and numerical simulations for a stage-structured predator–prey system (Li and Li, 2012) with Holling type-III response and time delay. Using a modified Holling type-II functional response, the stability of a two-dimensional prey-predator system with dual delays (Dubey et al., 2019) is investigated. Additionally, the implications of habitat complexity and prey refuge are explored. In this study, the stability and Hopf bifurcations in stage-structured predator-prey systems (Wei and Fu, 2016) with Beddington-DeAngelis functional response are examined. Additionally, the effects of prey refuge are analyzed using characteristic equation analysis. By preventing the extinction of prey, supporting global cohabitation (Xiang et al., 2023), and creating complex dynamics, such as numerous periodic orbits and homoclinic loops, as demonstrated by the Holling-Tanner model, refuge plays an essential role in maintaining ecosystems stability. In this study, the complex dynamics (Wang et al., 2014) arising from the Allee effect in a predator-prey model are investigated. The findings of this study demonstrate instability, diffusion-driven instability, and a variety of pattern forms, such as stripes, spots, and stripe-hole mixtures. It has investigated a Lotka–Volterra predator–prey model incorporates cannibalism (Deng et al., 2019; Respondek et al., 2017). The findings indicate that cannibalism can stabilize or destabilize the system, thereby affecting the coexistence or extinction of species. This is contingent on the dynamics of the original system and the intensity of cannibalism (Christle et al., 2007).

Motivated by the aforementioned research, we investigate using a predator-prey mathematical model the intricate interaction between academic stress and student well-being. Academic pressure rises alongside concerns about student mental health, fatigue, and performance. often, traditional explanations ignore system-level dynamics in favor of ecological, psychological, or sociological factors. This work fills that knowledge gap by simulating academic stress as the predator and students as the prey, thereby investigating how different stress levels affect student population stability. Understanding these dynamics is essential, as unbridled instabilities may drive the system into critical transitions or into chaos, necessitating quick intervention.

This study aims to systematically investigate the intricate interaction between the academic stress variable and the higher education student population. This work uses the Caputo fractional derivative in the context of predator-prey dynamics. Constructing a nonlinear mathematical model using differencing equations helps one assess the long-term effects of academic pressure on student stability. Furthermore, Lyapunov functions are used in a stability study of the equilibrium state to determine the number of equilibrium states and the stability of each one under several academic stresses. Numerical simulations allow one to investigate stress levels that produce changes in equilibrium. Hopf bifurcation, fold bifurcation, and flip bifurcation all influence the stress levels in educational systems that, over time, become unstable. Sensitivity analysis is used to ascertain how small variations in academic load could affect student population dynamics. The basin of attraction is thoroughly analyzed to identify initial conditions that lead to distinct long-term outcomes in the dynamics of academic stress and student populations. Analyzing sensitivity to initial conditions with Lyapunov exponents in the last stage reveals chaos and uncertainty. These contributions provide both theoretical and practical tools for developing long-term academic strategies.

Our current manuscript focuses on theoretical development and simulation-based insights due to limited access to longitudinal student stress datasets. The ABC fractional-order prey–predator model offers a refined framework for describing systems with long-term interdependencies, such as academic stress dynamics. Unlike traditional integer-order models, the ABC fractional-order derivatives add novelty by capturing memory effects that more accurately reflect how academic stress accumulates and affects student populations over time.

Formulation of the deterministic approach model

Using phase plane approaches, phase portraiture, numerical simulations, and stability analysis clarifies the dynamical behavior of the one- prey-one-predator model (Islam and Ahmed, 2024).This model (1) illustrates the predator-prey relationship between academic pressure (N_1), undergraduates (N_2) and graduate students (N_3) in higher education. The immense number of students enrolled in both the undergraduate and graduate programs makes academic pressure a formidable predator, causing stress and driving fierce competition for limited resources. Additionally, there is a feedback loop between the two groups of students, as the development of one group affects the pressures and scholastic requirements of the other. Academic pressure increases or decreases with student numbers, just as every population has its own intrinsic growth rate.

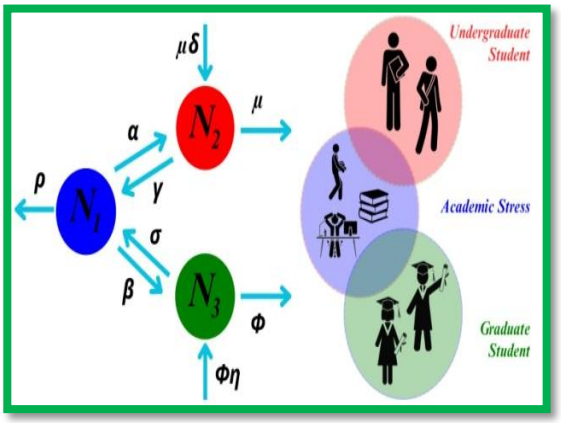

Fig. 1. Network diagram of the system with population states and transition pathways.

$$\begin{cases} \dfrac{dN_1}{dt} = \left(-\rho + \alpha N_2 + \beta N_3\right)N_1; \quad N_1(t) \geq 0 \\ \dfrac{dN_2}{dt} = \left(\mu(\delta - N_2) - \gamma N_1\right)N_2; \quad N_2(t) \geq 0 \\ \dfrac{dN_3}{dt} = \left(\phi(\eta - N_3) - \sigma N_1\right)N_3; \quad N_3(t) \geq 0 \end{cases} \tag{1}$$

As shown in Fig. 1, academic pressure is a predator that increases with student count but subsequently eliminates $(-\rho)$. The term $\alpha N_2 + \beta N_3$ describes the scenario whereby rising student enrolment results in a rise in rivalry for limited resources such as faculty, money, and research possibilities, therefore generating an increase in academic pressure (N_1). Constraints in resources including space, money, and faculty are causing the enrolment to be slowing down as it approaches capacity (δ). The sign $\mu(\delta - N_2)$ shows this. Referred to as $-\gamma N_1 N_2$, the loss of undergraduate students due to academic pressure (N_1) can cause stress, failures, and school dropout. The tenacity of undergraduates decreases in a predator-prey interaction as pressure (N_1). increases. A logistic growth model is used to characterize graduate students; $\phi(\eta - N_3)$ represents this model. The growth rate slows down to consider the limited resources when N_3 gets closer to its maximum. The theory of $-\alpha N_1 N_3$ explains how academic pressure N_1 can have a detrimental effect on graduate students (N_3), therefore causing burnout, delayed graduation, or a lack of willingness to continue their studies. Consistent with the predator-prey dynamic, a drop in N_3 results from an increase in N_1. A numerical measure of how rapidly academic pressure (N_1) influences graduate student retention rate (N_3), is captured by the coefficient α.

Table 1. The model description of parameters.

Parameter	Parameter Description	Parameter	Parameter Description
N_1	Predator: The population of predator which is academic pressure	α and β	Efficiency of academic pressure affecting undergraduate students and graduate students.
N_2	Prey 1: The population of undergraduate students	δ and η	Carrying capacities of the environment for undergraduate students and graduate students.
N_3	Prey 2: The population of graduate students	γ and σ	These could represent dropout rates for undergraduate students and graduate studentsdue to *a*cademic pressure.
ρ	The reduction rate for academicpressure	μ and λ	The factors that encourage an increase in student numbers.

Table 2. Initial values of parameters for α, β, γ, σ, μ.

Parameter	Values*	Parameter	Values**
α	0.02	σ	0.03
β	0.02	μ	0.01
γ	0.01		

Data source:*Tuerxun et al., 2020;**Wang et al., 2025

Local stability analysis of the model

A system of nonlinear equations (1) is first considered. The first aim is to find out the equilibrium points. For this purpose, set

$$P = (-\rho + \alpha N_2 + \beta N_3)N_1 = 0$$
$$Q = (\mu(\delta - N_2) - \gamma N_1)N_2 = 0$$
$$R = (\phi(\eta - N_3) - \sigma N_1)N_3 = 0$$

$$(u_0, v_0, w_0) = \{(0,0,0), (\frac{\mu\phi(\delta\alpha - \rho + \eta\beta)}{\gamma\alpha\phi + \sigma\beta\mu}, \frac{\gamma\rho\phi + \delta\sigma\beta\mu - \eta\gamma\beta\phi}{\gamma\alpha\phi + \sigma\beta\mu}, \frac{\sigma\rho\mu - \delta\sigma\alpha\mu + \eta\gamma\alpha\phi}{\gamma\alpha\phi + \sigma\beta\mu}),$$
$$(0,\delta,0), (0,0,\eta), (0,\delta,\eta), (\frac{-\mu(\rho - \delta\alpha)}{\gamma\alpha}, \frac{\rho}{\alpha}, 0), (\frac{-\phi(\rho - \eta\beta)}{\sigma\beta}, 0, \frac{\rho}{\beta})\}$$

The Jacobian matrix is defined as

$$J_{(u,v,w)} = \begin{pmatrix} P_{N_1} & P_{N_2} & P_{N_3} \\ Q_{N_1} & Q_{N_2} & P_{N_3} \\ R_{N_1} & R_{N_2} & R_{N_3} \end{pmatrix}$$

Where, $P = (-\rho + \alpha N_2 + \beta N_3)N_1$, $Q = (\mu(\delta - N_2) - \gamma N_1)N_2$, and $R = (\phi(\eta - N_3) - \sigma N_1)N_3$. Now differentiation of both P, Q and R with respect to N_1, N_2 and N_3 respectively and the Jacobian matrix is

$$J_{(u,v,w)} = \begin{pmatrix} \alpha N_2 - \rho + \beta N_3 & \alpha N_1 & \beta N_1 \\ -\gamma N_2 & \mu(\delta - 2N_2) - \gamma N_1 & 0 \\ -\sigma N_3 & 0 & \phi(\eta - 2N_3) - \delta N_1 \end{pmatrix}$$

Suppose $N_1 = u_0, N_2 = v_0, N_3 = w_0$
This yields the equilibrium points

Case 1: For the fixed point **(0,0,0)**

$$J_{(0,0,0)} = \begin{pmatrix} -\rho & 0 & 0 \\ 0 & \delta\mu & 0 \\ 0 & 0 & \eta\phi \end{pmatrix}$$

In this case, the eigenvalues are $-\rho$, $\delta\mu$ and $\eta\phi$, which are real; one is negative and the other two are positive. Then $(0,0,0)$, the trivial equilibriums always unstable.

Case 2: For the fixed point

$$(\frac{\mu\phi(\delta\alpha-\rho+\eta\beta)}{\gamma\alpha\phi+\sigma\beta\mu},\frac{\gamma\rho\phi+\delta\sigma\beta\mu-\eta\gamma\beta\phi}{\gamma\alpha\phi+\sigma\beta\mu},\frac{\sigma\rho\mu-\delta\sigma\alpha\mu+\eta\gamma\alpha\phi}{\gamma\alpha\phi+\sigma\beta\mu}),$$

$$J=\begin{pmatrix} p^* & \frac{\alpha\mu\phi(\delta\alpha-\rho+\eta\beta)}{\gamma\alpha\phi+\sigma\beta\mu} & \frac{\beta\mu\phi(\delta\alpha-\rho+\eta\beta)}{\gamma\alpha\phi+\sigma\beta\mu} \\ -\frac{\gamma(\gamma\rho\phi+\delta\sigma\beta\mu-\eta\gamma\beta\phi)}{\gamma\alpha\phi+\sigma\beta\mu} & q^* & 0 \\ -\frac{\sigma(\sigma\rho\mu-\delta\sigma\alpha\mu+\eta\gamma\alpha\phi}{\gamma\alpha\phi+\sigma\beta\mu} & 0 & r^* \end{pmatrix}$$

Where $p^*=\frac{\beta(\sigma\rho\mu-\delta\sigma\alpha\mu+\eta\gamma\alpha\phi)}{\gamma\alpha\phi+\sigma\beta\mu}-\rho+\frac{\alpha(\gamma\rho\phi+\delta\sigma\beta\mu-\eta\gamma\beta\phi}{\gamma\alpha\phi+\sigma\beta\mu}$,

$q^*=\mu(\delta-\frac{\alpha\rho\phi+\delta\sigma\beta\mu-\eta\gamma\beta\phi}{\gamma\alpha\phi+\sigma\beta\mu})-\mu\frac{\gamma\rho\phi+\delta\beta\sigma\mu-\eta\gamma\beta\phi}{\gamma\alpha\phi+\sigma\beta\mu}-\frac{\gamma\mu(\delta\alpha\phi-\rho\phi+\eta\beta\phi)}{\gamma\alpha\phi+\sigma\beta\mu}$

and

$r^*=\phi(\eta-\frac{\sigma\rho\mu-\delta\sigma\mu+\eta\gamma\alpha\phi}{\eta\gamma\alpha\phi})-\frac{\phi(\sigma\rho\mu-\delta\sigma\alpha\mu+\eta\gamma\alpha\phi)}{\gamma\alpha\phi+\sigma\beta\mu}-\frac{\sigma\mu(\delta\alpha\phi-\rho\phi+\eta\beta\phi)}{\gamma\alpha\phi+\sigma\beta\mu}$

The eigenvalue in the general form is very complicated to find in this case.

Case 3: For the fixed point $(0,\delta,0)$

$$J_{(0,\delta,0)}=\begin{pmatrix}\delta\alpha-\rho & 0 & 0\\ \delta\gamma & -\delta\mu & 0\\ 0 & 0 & \eta\phi\end{pmatrix}$$

In this case, the eigenvalues are $\delta\alpha-\rho$, $-\delta\mu$ and $\eta\phi$, which are real: one is negative, and the other two are positive. Therefore, $(0,\delta,0)$ is an unstable point.

Case 4: For the fixed point $(0,0,\eta)$

$$J_{(0,0,\eta)}=\begin{pmatrix}\eta\beta-\rho & 0 & 0\\ 0 & \delta\mu & 0\\ -\eta\beta & 0 & -\eta\phi\end{pmatrix}$$

In this case, the eigenvalues are $\eta\beta-\rho$, $\delta\mu$ and $-\eta\phi$, which are real: one is negative, and the other two are positive, since all the constants are positive. Therefore, $(0,0,\eta)$ is an unstable point. Here two eigenvalues are complex and one is real. Hence, it is a stable spiral for the complex values.

Case 5: For the fixed point $(0,\delta,\eta)$

$$J_{(0,\delta,\eta)}=\begin{pmatrix}\delta\alpha-\rho+\eta\beta & 0 & 0\\ -\delta\gamma & -\delta\mu & 0\\ -\eta\sigma & 0 & -\eta\phi\end{pmatrix}$$

In this case, the eigenvalues are $\delta\alpha-\rho+\eta\beta$, $-\delta\mu$ and $-\eta\phi$, which are real: one is negative and the other two are positive, since all the constants are positive.Since the real value is negative and real parts of the eigen values are also negative. Hence, $(0,\delta,\eta)$ is an unstable point.

Case 6: For the fixed point $(\frac{-\mu(\rho-\delta\alpha)}{\gamma\alpha},\frac{\rho}{\alpha},0)$

$$J_{(\frac{-\mu(\rho-\delta\alpha)}{\gamma\alpha},\frac{\rho}{\alpha},0)}=\begin{pmatrix}0 & \frac{-\mu(\rho-\delta\alpha)}{\gamma} & -\frac{\beta\mu(\rho-\delta\alpha)}{\gamma\alpha}\\ -\frac{\gamma\rho}{\alpha} & -\frac{\rho\mu}{\alpha} & 0\\ 0 & 0 & \eta\phi+\frac{\sigma\mu(\rho-\delta\alpha)}{\gamma\alpha}\end{pmatrix}$$

In this case the eigenvalues are

$-\frac{\rho\mu+\sqrt{\rho\mu(-4\delta\alpha^2+4\rho\alpha+\rho\mu)}}{2\alpha}$,

$\frac{\sigma\rho\mu-\delta\sigma\alpha\mu+\eta\gamma\alpha\phi}{\gamma\alpha}$ and $-\frac{\rho\mu-\sqrt{\rho\mu(-4\delta\alpha^2+4\rho\alpha+\rho\mu)}}{2\alpha}$. If the discriminant $\rho\mu(-4\delta\alpha^2+4\rho\alpha+\rho\mu)\geq 0$ then 2 of the eigenvalues are negative and, one is positive. Therefore, $(\frac{-\mu(\rho-\delta\alpha)}{\gamma\alpha},\frac{\rho}{\alpha},0)$ is an unstable point. On the other hand, if $\rho\mu(-4\delta\alpha^2+4\rho\alpha+\rho\mu)<0$ then two of the eigenvalues are complex and one is real. Real part of the eigenvalues is negative, but the real eigenvalue is positive, which are real and one of them is negative and the other two is positive. Hence, $(\frac{-\mu(\rho-\delta\alpha)}{\gamma\alpha},\frac{\rho}{\alpha},0)$ is an unstable point.

Case 7: For the fixed point $(\frac{-\phi(\rho-\eta\beta)}{\sigma\beta},0,\frac{\rho}{\beta})$

$$J_{(\frac{-\phi(\rho-\eta\beta)}{\sigma\beta},0,\frac{\rho}{\beta})}=\begin{pmatrix}0 & -\frac{\alpha\phi(\rho-\eta\beta)}{\sigma\beta} & -\frac{\phi(\rho-\eta\beta)}{\sigma}\\ 0 & \frac{\delta\mu+\gamma\phi(\rho-\eta\beta)}{\sigma\beta} & 0\\ -\frac{\sigma\rho}{\beta} & 0 & -\frac{\rho\phi}{\beta}\end{pmatrix}$$

In this case, the eigenvalues are

$-\frac{\rho\phi+\sqrt{\rho\phi(-4\eta\beta^2+4\rho\beta+\rho\phi)}}{2\beta}$, $\frac{\gamma\rho\phi+\delta\sigma\beta\mu+\eta\gamma\beta\phi}{\sigma\beta}$

and $-\frac{\rho\phi-\sqrt{\rho\phi(-4\eta\beta^2+4\rho\beta+\rho\phi)}}{2\beta}$. If the discriminate $\rho\phi(-4\eta\beta^2+4\rho\beta+\rho\phi)\geq 0$ then 2 of the eigenvalues are negative and, one is positive. Therefore, $(\frac{-\mu(\rho-\delta\alpha)}{\gamma\alpha},\frac{\rho}{\alpha},0)$ is an unstable point. On the other hand, if $\rho\phi(-4\eta\beta^2+4\rho\beta+\rho\phi)<0$ then two of the

eigenvalues are complex and one is real. Real part of the eigenvalues is negative, but the real eigenvalue is positive, which are real and one of them is negative, and the other two are positive. Hence, $(\frac{-\phi(\rho-\eta\beta)}{\sigma\beta},0,\frac{\rho}{\beta})$ is an unstable point.

Mathematical and dynamic analysis of the model

Positivity results

Theorem 1: Suppose $N_1(0)>0, N_2(0)>0, N_3(0)>0$.

The solutions $N_1(t), N_2(t), N_3(t)$ *remain positive for all* $N_2(t)$

Proof: From equation (1), we have

$\frac{dN_1}{dt}=(-\rho+\alpha N_2+\beta N_3)N_1$ *Set*, $-\rho+\alpha N_2+\beta N_3=\kappa$

Now,

$\frac{dN_1}{dt}=\kappa N_1 \Rightarrow \frac{dN_1}{N_1}=\kappa$

Integrating w.r.to t

$\int\frac{dN_1}{N_1}=\kappa\int dt \Rightarrow \ln N_1=\kappa t+C$

Where C is an arbitrary constant.

$\Rightarrow N_1=e^{\kappa t+C}$

$\Rightarrow N_1=e^{\kappa t}.e^{c}$

$\Rightarrow N_1(t)=C_1e^{\kappa t}$

Applying initial conditions $N_1(0)=N_{10}$

$\Rightarrow N_1(0)=C_1e^{0}\Rightarrow N_1(0)=C_1$

$\Rightarrow N_1(t)=N_1(0)e^{\theta t}$

The above expression depicts that $N_1(t)$ is nonnegative for all *t*. Similarly, $N_2(t)$ and $N_3(t)$ are positive for all $t\geq 0$.

Persistence of students populations

Theorem 2: The populations of undergraduate students (N_2) and graduate students (N_3) persist over time if academic pressure (N_1) does not exceed a critical threshold.

Proof: To prove Theorem 4.2 on the persistence of student populations, we need to analyze the conditions under which the populations of undergraduate students, N_2 and graduate students, N_3, remain positive over time, assuming initial values $N_1(0)>0, N_2(0)>0, N_3(0)>0$.

For $N_2>0$, we require: $\mu(\delta-N_2)\geq\gamma N_1$

Solving for N_1 we get a critical threshold:

$N_1\leq\frac{\mu(\delta-N_2)}{\gamma}$

Thus, for N_2 to persist over time, academic pressure, N_1 must remain below this threshold.

Conditions for N_3, the graduate population to remain positive

Similarly, N_3 to remain positive, it is required

$N_3'=(\phi(\eta-N_3)-\sigma N_1)N_3\geq 0$

$(\phi(\eta-N_3)-\sigma N_1)N_3\geq 0$

For $N_3>0$, it is required $(\phi(\eta-N_3))\geq\sigma N_1$

Solving for N_1 we get a critical threshold:

$N_1\leq\frac{\phi(\eta-N_3)}{\sigma}$

Thus, for N_3 to persist, academic pressure, N_1 must remain below this threshold.

For both N_2 and N_3 to positive simultaneously, we combine the two threshold conditions:

$N_1\leq\min\left(\frac{\mu(\delta-N_2)}{\gamma},\frac{\phi(\eta-N_3)}{\sigma}\right)$

The populations of undergraduate students (N_2) and graduate students (N_3) persist over time if academic pressure (N_1) does not exceed a critical threshold.

As shown in Fig. 2, Tables 1 and 2, with a decrease from 0.5 to nearly 0.2, academic pressure (N_1) remains near the critical threshold. Graduate (N_3) and undergraduate (N_2) populations grow over time by approximately 0.9 and 1.5 percentage points, respectively.

Basic reproduction number

In the present manuscript, the next-generation matrix approach is used to derive the basic reproduction number R_0, where the academic pressure variable N_1 is decomposed into stress-generation and stress-reduction components.

$F(N)$: Contributions to stress from students

$V(N)$: Outflows and damping of stress

$$\frac{dN1}{dt}=(-\rho+\alpha N_2+\beta N_3)N_1$$

$F(N)=(\alpha N_2+\beta N_3)N_1$ New stress sources

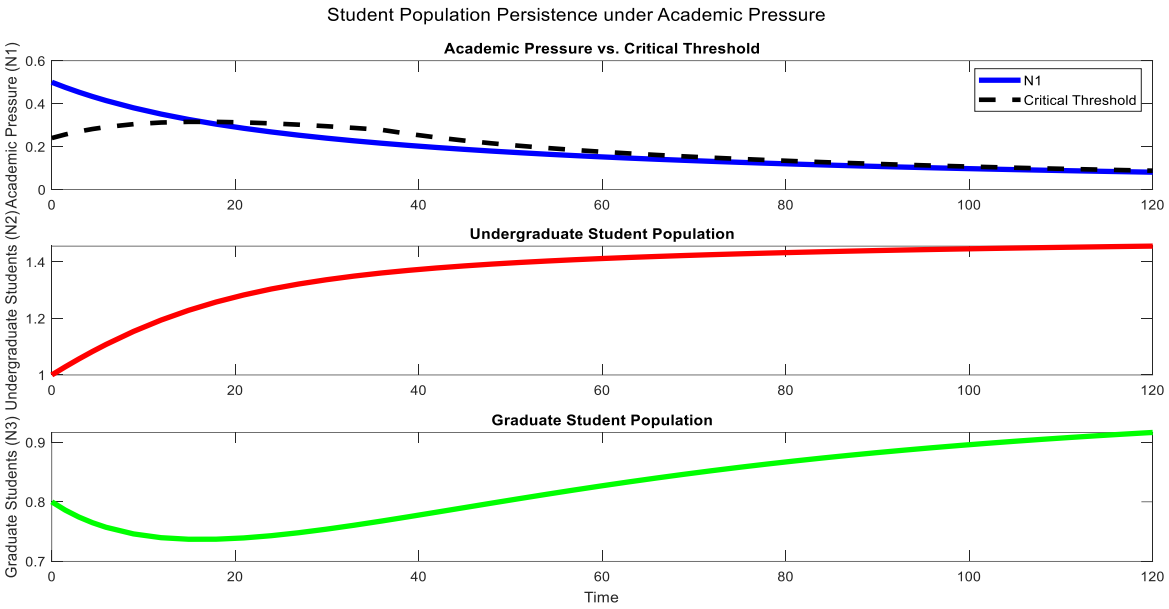

Fig. 2. The findings of the simulation show that the amount of academic pressure (N_1) on student populations varies around a key threshold.

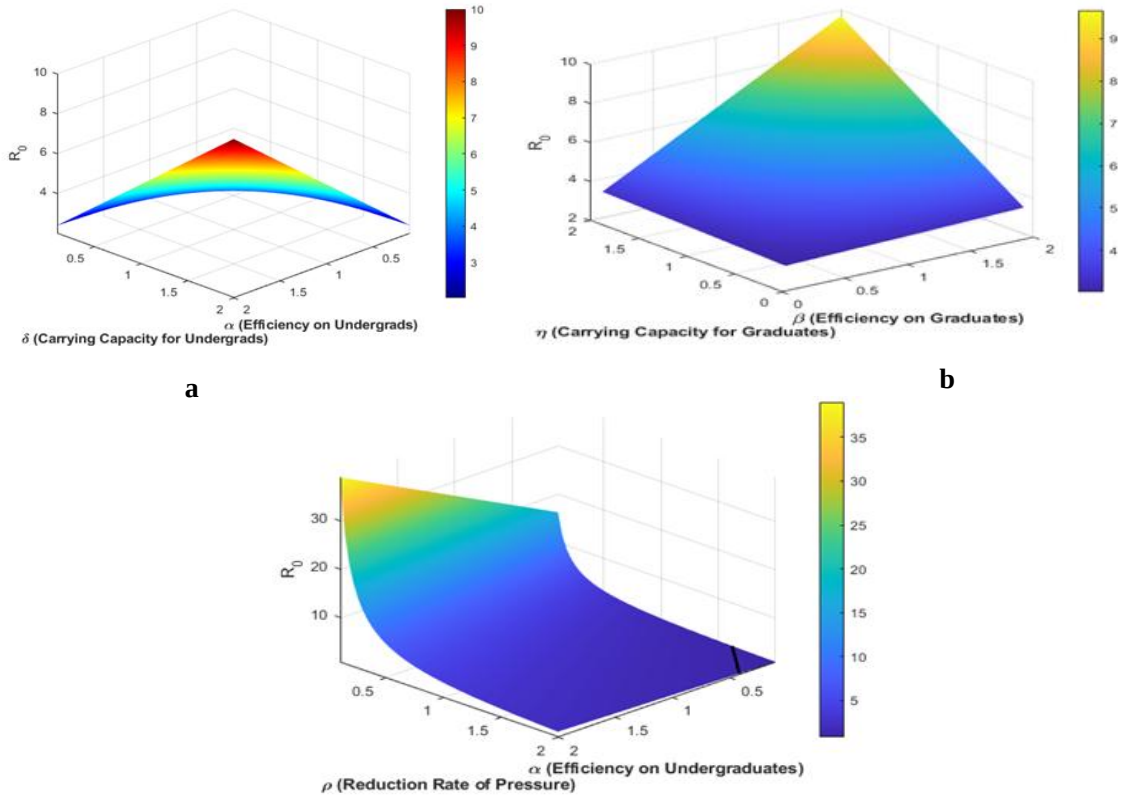

a **b**

c

Fig. 3. Effect of basic reproduction number (a) R_0 vs. α and δ, (b) R_0 vs. β and η, (c) R_0 vs. α and ρ.

$V(N) = \rho N_1$ Stress decay

$$F = \frac{\partial F(N)}{\partial N_1} = \frac{\partial}{\partial N_1}(\alpha N_2 + \beta N_3)N_1$$

$$F = \frac{\partial F(N)}{\partial N_1} = \alpha N_2 + \beta N_3$$

Stress-free equilibrium point, $N_1 = 0, N_2 = \delta, N_3 = \eta$

$$F = \alpha\delta + \beta\eta$$

$$V = \frac{\partial}{\partial N_1}V(N)$$

$$V = \frac{\partial}{\partial N_1}(\rho N_1) = \rho$$

$$V^{-1} = \frac{1}{\rho}$$

Next generation matrix

$$R_0 = FV^{-1}$$

$$R_0 = \frac{\alpha\delta+\beta\eta}{\rho} \qquad (2)$$

Fig. 3 show that R_0 increases with pressure efficiency (α, β) and carrying capacities(δ, η), but decreases sharply with a higher pressure reduction rate ρ, emphasizing its dominant control role.

Bifurcation analysis

Bifurcations mark locations within a system, at which the system shifts from one state to another, usually resulting in novel patterns, structures, and its dynamics.The characteristic matrix of (1) is

$$J - \lambda I = \begin{bmatrix} (-\rho + \alpha N_2 + \beta N_3) - \lambda & \alpha N_1 & \beta N_1 \\ -\gamma N_2 & (\mu(\delta - 2N_2) - \gamma N_1) - \lambda & 0 \\ -\sigma N_3 & 0 & (\phi(\eta - 2N_3) - \sigma N_1) - \lambda \end{bmatrix}$$

The characteristic equation is $|J - \lambda I| = 0$

$$\Rightarrow ((-\rho + \alpha N_2 + \beta N_3) - \lambda)[((\mu(\delta - 2N_2) - \gamma N_1) - \lambda)((\phi(\eta - 2N_3) - \sigma N_1) - \lambda)] -$$
$$\alpha N_1((-\gamma N_2))((\phi(\eta - 2N_3) - \sigma N_1) - \lambda) + \beta N_1[0 - [(-\sigma N_3)((\mu(\delta - 2N_2) - \gamma N_1) - \lambda)]] = 0$$

$$\Rightarrow ((-\rho + \alpha N_2 + \beta N_3) - \lambda)\begin{bmatrix} \mu(\delta - 2N_2)(\phi(\eta - 2N_3)) - \mu(\delta - 2N_2)\sigma N_1 - \mu\lambda(\delta - 2N_2) \\ -\gamma N_1(\phi(\eta - 2N_3)) - \gamma\sigma N_1{}^2 - \gamma\lambda N_1 - \lambda(\phi(\eta - 2N_3)) + \sigma\lambda N_1 + \lambda^2 \end{bmatrix}$$
$$-\alpha N_1[-\gamma N_2(\phi(\eta - 2N_3)) + \gamma\sigma N_1 N_2 + \gamma\lambda N_2] + \beta N_1[-[(-\sigma N_3)(\mu(\delta - 2N_2)) + \sigma\gamma N_1 N_2 + \sigma\lambda N_3]] = 0$$

$$\Rightarrow ((-\rho + \alpha N_2 + \beta N_3) - \lambda)\begin{bmatrix} (\mu\delta - 2\mu N_2)(\phi\eta - 2\phi N_3) - \mu\delta\sigma N_1 + 2\mu\sigma N_1 N_2 - \mu\lambda\delta \\ 2\mu\lambda N_2 - \gamma N_1(\phi\eta - 2\phi N_3) - \gamma\sigma N_1{}^2 - \gamma\lambda N_1 - \lambda\phi\eta + 2N_3\lambda \\ \sigma\lambda N_1 + \lambda^2 \end{bmatrix} -$$
$$\alpha N_1[-\gamma N_2\phi\eta + 2\gamma N_2 N_3 + \gamma\sigma N_1 N_2 + \gamma\lambda N_2] + \beta N_1[\sigma\mu\delta N_3 - 2\sigma N_2 N_3 + \sigma\gamma N_1 N_2 + \sigma\lambda N_3] = 0$$

$$\Rightarrow -\lambda^3 + A\lambda^2 + B\lambda + C = 0$$

$$\Rightarrow \lambda^3 - A\lambda^2 - B\lambda - C = 0 \qquad (3)$$

Where, $A = (-\rho + \alpha N_2 + \beta N_3 + \mu\delta - 2\mu N_2 + \gamma N_1 + \phi\eta - 2N_3 - \sigma N_1)$.

$B = (\mu\rho\delta - 2\rho\mu + \rho\gamma N_1 + \rho\phi\eta -$
$-2\rho N_3 - \rho\sigma N_1 - \alpha\mu\delta N_2 + 2\alpha\mu N_2{}^2 - \alpha\gamma N_1 N_2 - \alpha\phi\eta N_2 + 2\alpha N_2 N_3 + \alpha\sigma N_1 N_2 - \mu\beta\delta +$
$2\beta\mu N_2 N_3 - \beta\rho\gamma N_1 N_3 - \beta\phi\eta N_3 + 2\beta\rho N_3{}^2 + \beta\sigma N_1 N_3 - \mu\delta\phi\eta + 2\mu\delta\phi N_3 + 2\mu\phi\eta N_2 - 4\mu\phi N_2 N_3 + \mu\delta\sigma N_1$
$-2\mu\sigma N_1 N_2 + \gamma\phi\eta N_1 - 2\phi\gamma N_1 N_2 + \gamma\sigma N_1{}^2 - \alpha\gamma N_1 N_2 + \beta\sigma N_1 N_2)$.

$C = (2\rho\mu\delta\phi N_3 - \rho\mu\delta\phi\eta + 2\mu\rho\phi\eta N_2 -$
$4\rho\mu\phi N_2 N_3 + \rho\mu\delta\sigma N_1 - 2\rho\mu\sigma N_1 N_2 + \rho\gamma\phi\eta N_1 - 2\rho\phi\gamma N_1 N_3 + \rho\gamma\sigma N_1{}^2 + \alpha\mu\delta\phi\eta N_2 - 2\alpha\mu\delta\phi N_2 N_3 -$
$2\alpha\mu\phi\eta N_2{}^2 + 4\alpha\mu\phi N_2{}^2 N_3 - \alpha\mu\delta\sigma N_1 N_2 + 2\alpha\mu\sigma N_1 N_2{}^2 - \alpha\gamma\phi\eta N_1 N_2 + 2\alpha\phi\gamma N_1 N_2 N_3 - \alpha\gamma\sigma N^{1^2} N_2$
$+ \beta\mu\delta\phi\eta N_3 - 2\beta\mu\delta\phi N_3{}^2 - 2\mu\beta\rho\phi\eta N_2 N_3 + 4\beta\mu\phi N_2 N_3{}^2 - \beta\rho\mu\delta\sigma N_1 N_3 + 2\beta\mu\sigma N_1 N_2 N_3$
$- \beta\gamma\phi\eta N_1 N_3 + 2\beta\phi\gamma N_1 N_3{}^2 - \beta\gamma\sigma N_1{}^2 N_3 + \alpha\gamma\phi\eta N_1 N_2 - 2\alpha\gamma N_1 N_2 N_3 - \alpha\gamma\sigma N_1{}^2 N_2 + \beta\sigma\mu\delta N_1 N_2$
$- 2\beta\sigma N_1 N_2 N_3 + \beta\sigma\gamma N_1{}^2 N_3 - 2\beta\sigma N_1 N_2 N_3 + \beta\sigma\gamma N_1{}^2 N_3)$.

Fold bifurcation

In a prey-predator model with student populations and academic stress, a fold bifurcation occurs as from parameter is varied, leading to two equilibrium points: one stable and one unstable, which converge and then destroy. Little changes in stressful circumstances have caused the system to shift from a stable to an unstable stress state. For fold bifurcation (Islam et al., 2025; Zheng et al., 2018) $\lambda = 1$, then the equation (3) becomes

$$\Rightarrow 1^3 - A.1^2 - B.1 - C = 0$$
$$\Rightarrow A + B + C = 1$$

Flip bifurcation

Through the flip bifurcation of the student-prey-predator model incorporating academic stress, a better understanding of how increasing stressor intensity might influence students' stress levels, thereby transforming them from stable to oscillatory or even chaotic. This phenomenon increases the risk of burnout, inefficiency, and erratic academic performance for students. For fold bifurcation (Islam et al., 2025; Zheng et al., 2018) $\lambda = -1$, then the equation (3) becomes

$$\lambda^3 - A\lambda^2 - B\lambda - C = 0$$
$$-1 - A + B - C = 0$$
$$\Rightarrow A - B + C = -1$$

Hopf bifurcation

There are some Hopf bifurcations in a prey-predator model of student populations regarding academic stress, which lay the foundations of understanding transitions between equilibrium and periodic behavior. With increasing stress, the system can transition from a steady-state stress that can be managed to periodic oscillations, in which stress levels fluctuate. These oscillations are stable or unstable depending on the nature of the Hopf bifurcation: supercritical or subcritical. This analysis reveals how minor variations in stress can lead to dramatic changes in student behavior and health, thereby affecting how students deal with academic tests.

Theorem 3: The system (1) exhibits a Hopf bifurcation when the reduction rate for academic pressure, indicated as ρ, approaches a critical value designated as ρ_c. This results in the characteristic equation exhibiting a pair entirely imaginary eigenvalues $\lambda = \pm i\omega$. The existence of $\rho = \rho_c$ such a Hopf bifurcation (Sha et al., 2019) can occur under some conditions.

(i) The equation (3) has a pair of purely imaginary roots $\lambda = \pm i\omega$.

(ii) The real part of eigenvalues sign as ρ varies, i.e.

$$\frac{d}{d\rho}\mathrm{Re}(\lambda(\rho))\Big|_{\rho=\rho_c} \neq 0$$

Proof: At $\boldsymbol{\rho = \rho_c}$, for the Hopf bifurcation $\lambda = \pm i\omega$, equation (3) becomes

$$(i\omega)^3 - A(i\omega)^2 - B(i\omega) - C = 0$$
$$\Rightarrow -i\omega^3 + A\omega^2 - Bi\omega - C = 0$$

Equating the real and imaginary parts as follows,

$$\Rightarrow A\omega^2 - C = 0$$
$$\Rightarrow \omega^2 = \frac{C}{A}$$
$$(-i\omega)^3 - A(-i\omega)^2 - B(-i\omega) - C = 0$$
$$\Rightarrow -i^3\omega^3 - Ai^2\omega^2 + Bi\omega - C = 0$$
$$\Rightarrow i\omega^3 + A\omega^2 + i\omega - C = 0$$

Equating the real and imaginary parts as follows,

$$\Rightarrow A\omega^2 - C = 0$$
$$\Rightarrow \omega^2 = \frac{C}{A}$$

Where ω the frequency at the purely imaginary eigenvalues occurs.

Imaginary part:

$$-\omega^3 - \rho\omega = 0 \Rightarrow \omega^3 + \rho\omega = 0 \Rightarrow \omega(\omega^2 + \rho) = 0$$

Since $\omega \neq 0$, it follows that: $B + \omega^2 = 0 \Rightarrow B = -\omega^2$ (4)

From the real part equation $\omega^2 = \frac{C}{A}$

From equations (4) and (5) for ω^2: $B = -\frac{C}{A}$

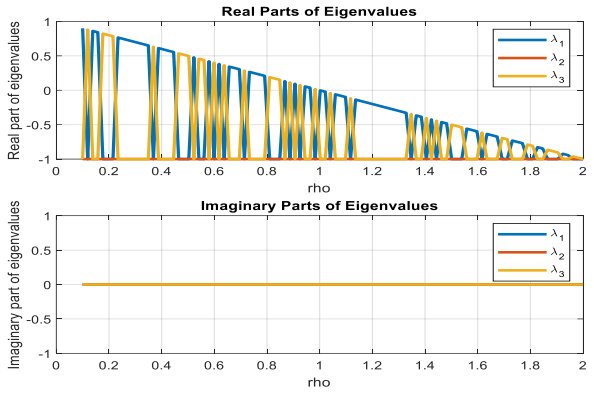

Fig. 4. Hopf bifurcation in academic dynamics showing stability transitions via eigenvalues.

For a Hopf bifurcation to occur, it is needed

$$B(\rho_c) = -\frac{C(\rho_c)}{A(\rho_c)}$$

It is verified that the transversality condition holds. To ensure that the eigenvalues cross the imaginary axis transversely, it is computed $\frac{d}{d\rho}\mathrm{Re}(\lambda(\rho))\Big|_{\rho=\rho_c}$

Differentiating (3) with respect to ρ

$$3\lambda^2\frac{d\lambda}{d\rho} - 2A\lambda\frac{d\lambda}{d\rho} - A'\lambda^2 - B'\lambda - C' = 0 \qquad (6)$$

ing the real and imaginary parts for $\lambda = i\omega$

$$3(i\omega)^2\frac{d\lambda}{d\rho} - 2A(i\omega)\frac{d\lambda}{d\rho} - A'(i\omega)^2 - B'(i\omega) - C' = 0$$

$$\Rightarrow 3(-\omega^2)\frac{d\lambda}{d\rho} - 2Ai\omega\frac{d\lambda}{d\rho} + A'\omega^2 - iB'\omega - C' = 0$$

Real part; $3\omega^2\frac{d\lambda}{d\rho} + A'\omega^2 - C' = 0$

Imaginary part: $-2A\omega\frac{d\lambda}{d\rho} - B'\omega = 0$

$$\Rightarrow \frac{d\lambda}{d\rho}(\upsilon) = -\frac{B'(\rho)}{2A(\rho)} \text{ and } \frac{d}{d\rho}\mathrm{Re}(\lambda(\rho))\Big|_{\rho=\rho_c} \neq 0$$

This means that the transversality criterion holds. This leads one to assume that the point $\rho = \rho_c$ is the location of a Hopf bifurcation. This ends the proof of the theorem.

The actual eigenvalues consist beyond zero at $\rho = 1.2$.

When the equilibrium point shifts to an unstable, limit cycle, also known as a periodic solution results. Here lies theHopf bifurcation point. If $\rho > 1.2$ the real componentsof the eigenvaluesare positive. The system shows fluctuating behavior; the equilibrium point is unstable. The Hopf bifurcation point is found at $\rho = 1.2$, at which the system shifts from stable to unstable behavior and limit cycles appear. The fact that ρ changes from stable to unstable as it develops suggests that excessive academic pressure may drive the system toward instability

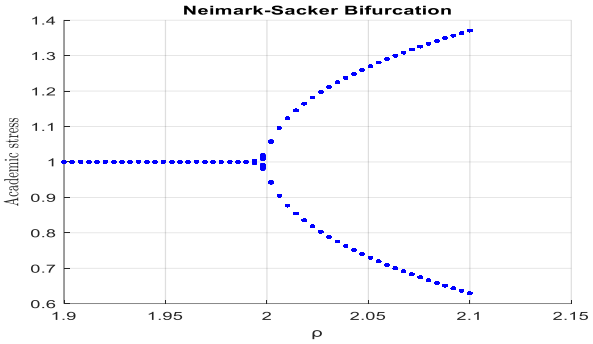

Fig. 5. Neimark-Sacker bifurcation in academic stress dynamics using the model.

Neimark-Sacker bifurcation

In discrete conditions, a bifurcation analogous to the Hopf bifurcation occurs; this one is called the Neimark-Sacker bifurcation. Although the same conclusion as Neimark, they did so independently. Upon first examination, the idea was determined to be consistent with periodic solution stability by Asheghi Sacker. The first place it appears in ordinary differential equations is in the map obtained by taking a Poincare section perpendicular to the periodic flow. One often used discretization method for the systems:

$$N_i(t+h) = N_i(t) + hf_i(N_1, N_2, N_3)$$

Where *h*is the step size. Applying this, the system transforms into:

$$N_1^{k+1} = N_1^k + h(-\rho + \alpha N_2^k + \beta N_3^k)N_1^k$$
$$N_2^{k+1} = N_2^k + h(\mu(\delta - N_2^k) - \gamma N_1^k)N_2^k$$
$$N_3^{k+1} = N_3^k + h(\phi(\eta - N_3^k) - \sigma N_1^k)N_3^k$$

A Neimark-Sacker bifurcation is the result of a complex-conjugate pair of eigenvalues crossing the unit circle, indicating that the system (3) is unstable if at least one eigenvalue is found outside the unit circle, denoted as $|\lambda i| > 1$. $\lambda_{1,2} = \pm e^{i\theta}$, $0 < \theta < \pi$

The system (3) is stable if all eigenvalues satisfy $|\lambda i| < 1$. The Jury stability conditions are:

(i) $1 + A + B + C > 0$
(ii) $1 - A + B - C > 0$
(iii) $A - C > 0$
(iv) $|C| < 1$

When the condition $A - C = 0$ is met, a Neimark-Sacker bifurcation occurs, as a pair of complex eigenvalues moves to the unit circle. The bifurcation occurs when two of the eigenvalues of equation (3) satisfy: $\lambda_{1,2} = \pm e^{i\theta}$. For this to hold, substitute $\lambda = e^{i\theta}$ in the equation (3), $\left(e^{i\theta}\right)^3 - A\left(e^{i\theta}\right)^2 - B\left(e^{i\theta}\right) - C = 0$
Splitting the real and imaginary parts, this gives conditions for A, B, and C in terms of the bifurcation parameters.

Variations in the bifurcation parameter ρ affect the level of academic stress displayed in the bifurcation indicated in Fig.5. A stable fixed point may shift in a Neimark-Sacker bifurcation into an unstable point prone to oscillation. Rather than displaying a continuous condition close to the Neimark-Sacker bifurcation at ρ≈2, academic stress is determined by periodic fluctuations or oscillations. This result has significant relevance for evaluating student stress levels across both academic and non-academic domains.

The real and imaginary components of the eigenvalues $(\lambda_1, \lambda_2, \lambda_3)$ for varying bifurcation parameter α are displayed in Table 3. One finds a transition from steady to oscillatory behavior as αrises. Two complex conjugate eigenvalues crossing the unit circleand generating quasiperiodic oscillations define a bifurcation near 1.3. When the imaginary components approach 1.3, the system becomes unstable and exhibits continuous oscillations beyond this threshold.

As an expression of the bifurcation parameter α the Fig. 6 shows the real and imaginary eigenvalues $(\lambda_1, \lambda_2, \lambda_3)$. Two complex conjugate eigenvalues crossing the unit circle causes the Neimark-Sacker bifurcation to move the system from stability to oscillation. Two complex conjugate eigenvalues cross the unit circle as α rises to produce oscillations reminiscent of a Neimark-Sacker bifurcation. The imaginary components of the eigenvalues show a transition from a stable to an oscillatory regime in the range $1.2 \le \alpha \le 1.5$. All eigenvalues are real and in the stability domain before α≈1.2, therefore guaranteeing system stability. The system becomes unstable at α≈1.5 because of oscillations reflecting Neimark-Scker bifurcations brought about by complex conjugate eigenvalues crossing the unit circle. Starting quasiperiodic behavior at α≈1.3, the critical bifurcation point arises when eigenvalues satisfy Jury stability conditions and depart the stability domain.

Fig. 7 shows the ROR values as afunction of ρ, the bifurcation value. The red dashed line defines the criteria for stable and unstable behavior; the computed ROR values are shown by the solid blue line. The ROR approach can find a closed invariant curve as a Neimark-Sacker bifurcation when an unstable

Table 3. Eigenvalue analysis and stability classification.

α	**Real Part** λ_1	**Imaginary Part** λ_1	**Real** Part λ_2	**Imaginary Part** λ_2	**Real Part** λ_3	**Imaginary Part** λ_3	**Stability Status**
1.0	0.8	0.0	0.5	0.0	-0.3	0.0	Stable
1.2	0.7	0.2	0.5	0.0	-0.2	-0.1	Stable
1.3	0.6	0.5	0.4	-0.2	-0.1	-0.2	Bifurcation
1.4	0.5	0.7	0.3	-0.3	0.0	-0.4	Unstable
1.5	0.4	0.9	0.2	-0.4	0.1	-0.5	Unstable
1.6	0.3	1.1	0.1	-0.5	0.2	-0.6	Unstable

fixed point results from it. ROR crossing $R=0$ shows a transition from stable to quasiperiodic oscillations. The ROR values exhibit initial fluctuations at reduced ρ levels but remain positive, suggesting a stable regime. The ROR values drop and oscillate near to the threshold as ρ rises. The ROR declining below zero at ρ≈1.4, indicating bifurcation. Decline in ROR values beyond ρ≈1.6 indicates the existence of instability and complicated dynamical behavior. The motion is quasiperiodic due to this Neimark-Sacker bifurcation, which marks the transition from regular dynamics to oscillatory motion.

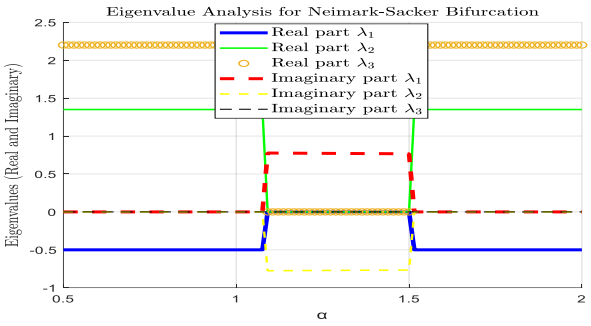

Fig. 6. Eigenvalue analysis for Neimark-Sacker bifurcation.

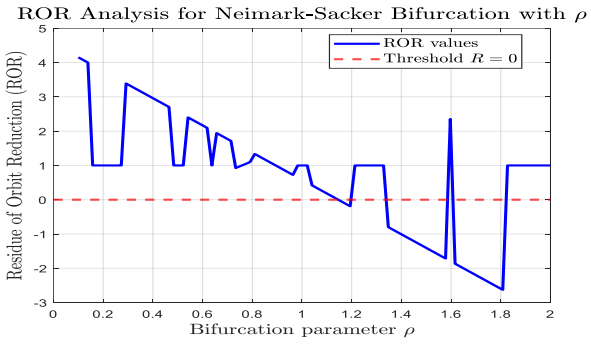

Fig. 7. Residue of orbit reduction (ROR) analysis for Neimark-Sacker bifurcation with *ρ*.

As shown in table 4, the Neimark-Sacker bifurcation occurs at ρ≈1.4 when the ROR value crosses the zero criteria. The system exhibits more unstable oscillations when the threshold is crossed.

Global stability

Let us consider N_1 (8)

Table 4. Stability classification based on residue of orbit reduction (ROR) analysis.

ρ	ROR Value	Stability Status
0.2	3.8	Stable
0.6	2.5	Stable
1.0	0.9	Stable
1.2	0.3	Stable
1.4	-0.2	Bifurcation point
1.6	-1.5	Unstable
1.8	-2.3	Unstable

Where $a,b,c>0$ are positive constants.

$$\frac{dV}{dt} = 2a(N_1 - N_1^*)\acute{N}_1 + 2b(N_2 - N_2^*)\acute{N}_2 + 2c(N_3 - N_3^*)\acute{N}_1$$

From $\frac{dV}{dt} = 2a(N_1 - N_1^*)\acute{N}_1 + 2b(N_2 - N_2^*)\acute{N}_2 + 2c(N_3 - N_3^*)\acute{N}_1$

Substituting the given system equations:

$$\frac{dV}{dt} = 2a(N_1 - N_1^*)(-\rho + \alpha N_2 + \beta N_3)N_1 + 2b(N_2 - N_2^*)(\mu(\delta - N_2) - \gamma N_1)N_2 + 2c(N_3 - N_3^*)(\phi(\eta - N_3) - \sigma N_1)N_3 \quad (9)$$

Since we assume that the system has an equilibrium

$$-\rho + \alpha N_2 + \beta N_3 = 0$$

$$2b(N_2 - N_2{}^*)(\mu(N_2{}^* - N_2) - \gamma(N_1 - N_1{}^*))N_2$$

At equilibrium $\mu(\delta - N_2) - \gamma N_1 = 0$

So we write

$$2b(N_2 - N_2{}^*)(\mu(N_2{}^* - N_2) - \gamma(N_1 - N_1{}^*))N_2$$

Since $\mu(N_2{}^* - N_2)$ is negative definite, this term contributes to making $\frac{d\Psi}{dt} \le 0$.

$$2c(N_3 - N_3{}^*)(\phi(\eta - N_3) - \sigma N_1)N_3$$

$$\phi(\eta - N_3{}^*) - \sigma N_1{}^*$$

Rewriting

$$2c(N_3 - N_3{}^*)(\phi(N{}^* - N_3) - \sigma(N_1 - N_1{}^*))N_3$$

Since $\frac{dV}{dt} \leq 0$, also $\frac{dV}{dt} = 0$ only at equilibrium point $(N_1{*}, N_2{*}, N_3{*})$. LaSalle's invariance principle guarantees the global asymptotic stability of the equilibrium.

It appears from Fig. 8 that the globally stable equilibrium point is at (N_1, N_2, N_3) = (250, 10, 8), as all paths from many starting locations converge to this point and the Lyapunov function monotonically decreases to zero. The oscillatory character of the phase images indicates that the system undergoes transitory oscillations before reaching a stable state. This is typical of real-world academic systems that apply feedback. The Lyapunov function mathematically ensures stability since it is usually zero over time. This suggests that although the system would eventually settle, academic pressure on students would induce transient changes in the population.

Fractional order approach

Definition 1. Using the following formula, we can find the integral (Ullahand Kabir, 2024)that corresponds to $g(t)$in the ABC sense, assuming that it is a function on the interval L [0, T]:

$$ {}^{ABC}_{0}I_t^{\alpha} g(t) = \frac{1-v}{ABC(v)} g(t) + \frac{v}{ABC(v)\Gamma(v)} \int_0^t (t-\theta)^{v-1} g(\theta)\, d\theta \quad (10)$$

Lemma 1: In accordance with the information provided in reference(Ullah and Kabir, 2024), the third statement asserts that the optimal solution to the theoretical challenge with fractional order $0 < \alpha \leq 1$is

$${}^{ABC}_{0}D_t^{v} g(t) = y(t), t \in [0, T]$$

$$g(0) = g_0$$

On the basis of the fact that the right side disappears when time equals zero, then

$$g(t) = g_0 + \frac{1-v}{ABC(v)} y(t) + \frac{v}{ABC(v)\Gamma(v)} \int_0^t (t-\theta)^{v-1} y(\theta)\, d\theta \quad (11)$$

Fractional order model

The section that follows summarizes our analysis of a fractional-order student population model that employs the ABC fractional derivative (Ullah and Kabir, 2024). The model that preceded it (1) informs this part.

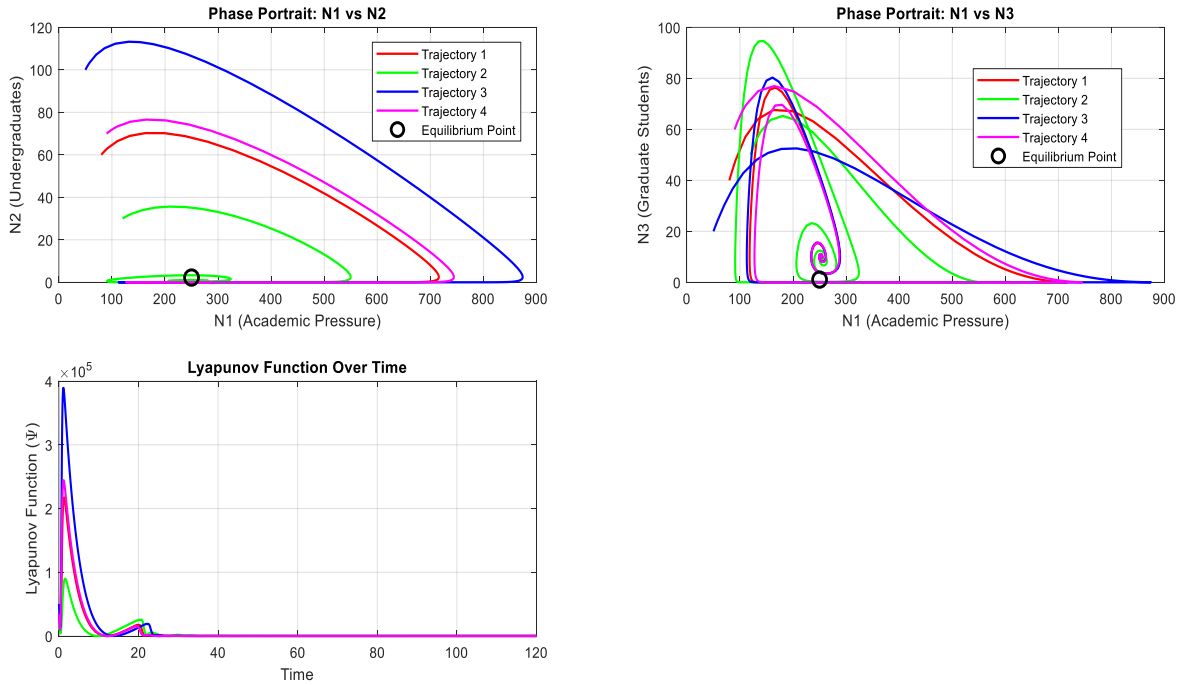

Fig. 8. Global stability analysis using phase portraits and Lyapunov function (8).

$$\left.\begin{array}{l} {}^{ABC}_{0}D_t^{v}[N_1(t)] = (-\rho + \alpha N_2 + \beta N_3)N_1 \\ {}^{ABC}_{0}D_t^{v}[N_2(t)] = (\mu(\delta - N_2) - \gamma N_1)N_2 \\ {}^{ABC}_{0}D_t^{v}[N_3(t)] = (\phi(\eta - N_3) - \sigma N_1)N_3 \end{array}\right\} \quad (12)$$

Under the initial values for the various classes

$N_1(0) \geq 0, N_2(0) \geq 0, N_3(0) \geq 0$

Boundedness of solutions

Theorem 4: Let $0 < \nu \leq 1$, and assume all parameters $\rho, \sigma, \alpha, \beta, \mu, \delta, \gamma, \phi, \eta$ are positive constants. Then, the solutions of the system (12) eventually enter the compact region $S = \left\{(N_1, N_2, N_3) \epsilon \Re_+^3 | g(t) \leq \delta + \frac{H}{N}, \delta > 0\right\}$ for some $N \leq \min\{\rho, \mu\delta, \phi\eta\}$ and a constant $H > 0$,

Proof: We define a function (Sha et al., 2019) as

$$g(t) = N_1(t) + N_2(t) + N_3(t),\ t \geq 0 \quad (13)$$

Take the ABC derivative:

$${}^{ABC}_{0}D_t^{v}g(t) = {}^{ABC}_{0}D_t^{v}N_1(t) + {}^{ABC}_{0}D_t^{v}N_2(t) + {}^{ABC}_{0}D_t^{v}N_3(t) \quad (14)$$

From equations (12), (13), and (14)

$$\begin{aligned} {}^{ABC}_{0}D_t^{v}N_1(t) &= (-\rho + \alpha N_2 + \beta N_3)N_1 \\ &\quad + (\mu(\delta - N_2) - \gamma N_1)N_2 \\ &\quad + (\phi(\eta - N_3) - \sigma N_1)N_3 \end{aligned}$$

$$\begin{aligned} \Longrightarrow {}^{ABC}_{0}D_t^{v}N_1(t) &= -\rho N_1 + \alpha N_1 N_2 + \beta N_1 N_3 \\ &+ \mu\delta N_2 - \mu N_2^2 - \gamma N_1 N_2 + \phi\eta N_3 - \phi N_3^2 - \sigma N_1 N_2 \end{aligned}$$

Simplify

$$\begin{aligned} \Longrightarrow {}^{ABC}_{0}D_t^{v}N_1(t) &= -\rho N_1 + (\alpha - \gamma)N_1 N_2 \\ &\quad + (\beta - \sigma)N_1 N_3 \\ &+ \mu\delta N_2 - \mu N_2^2 + \phi\eta N_3 - \phi N_3^2 \end{aligned}$$

Now adding a damping term $Ng(t)$, where $N \leq min\{\rho, \mu\delta, \phi\eta\}$

The total population$F(t)$ $is\ ultimately\ bounded$, hence the system solutions are bounded in the region S.

Existence and uniqueness of the solution for the fractional order model:

We determine whether the solutions to system (12) are unique with respect to the ABC derivative and whether they exist. Choosing into account that a continuous real-valued function with the supremum-norm assets is indicated as B (ς) on ς = [0, b] and P= B [ς]×B[ς]× B[ς](Ullah andKabir, 2024),the corresponding function is a component of a Banach space and with the norm $\|(N_1, N_2, N_3)\| = \|N_1\| + \|N_2\| + \|N_2\|$,

Whereas

$\|N_1\| = \sup_{t \in k}|N_1|, \|N_2\| = \sup_{t \in k}|N_2|, \|N_3\| = \sup_{t \in k}|N_3|$. What occurs is the outcome of applying the fractional integral operator of ABC to the two sets of equations (12):

$$\left.\begin{array}{l} N_1(t) - N_1(0) = {}^{ABC}_{0}D_t^{v}\{(-\rho + \alpha N_2 + \beta N_3)N_1\} \\ N_2(t) - N_2(0) = {}^{ABC}_{0}D_t^{v}\{(\mu(\delta - N_2) - \gamma N_1)N_2\} \\ N_3(t) - N_3(0) = {}^{ABC}_{0}D_t^{v}\{(\phi(\eta - N_3) - \sigma N_1)N_3\} \end{array}\right\} \quad (15)$$

With the ABC fractional derivative in hand, one arrives at the following:

$$\begin{cases} N_1(t) - N_1(0) = \frac{1-v}{ABC(v)} g_1(v, t, N_1(t)) + \frac{v}{ABC(v)\Gamma(v)} \int_0^t (t-\theta)^{v-1} g_1(v, t, N_1(\theta))\, d\theta \\ N_2(t) - N_2(0) = \frac{1-v}{ABC(v)} g_2(v, t, N_2(t)) + \frac{v}{ABC(v)\Gamma(v)} \int_0^t (t-\theta)^{v-1} g_2(v, t, N_2(\theta))\, d\theta \\ N_3(t) - N_3(0) = \frac{1-v}{ABC(v)} g_3(v, t, N_3(t)) + \frac{v}{ABC(v)\Gamma(v)} \int_0^t (t-\theta)^{v-1} g_3(v, t, N_3(\theta))\, d\theta \end{cases} \quad (16)$$

Where

$$\begin{aligned} &g_1(v, t, N_1(t)) = (-\rho + \alpha N_2 + \\ &\beta N_3)N_1,\ g_2(v, t, N_2(t)) = (\mu(\delta - N_2) - \\ &\gamma N_1)N_2,\ g_3(v, t, N_3(t)) = (\phi(\eta - N_3) - \sigma N_1)N_3 \end{aligned} \quad (17)$$

As used within the circumstances of $(t), N_2(t), N_3(t)$ the functions g_1, g_2, g_3 satisfy the Lipschitz condition if each of the three functions $N_1(t), N_2(t), N_3(t)$has an upper bound. Because of this,

$$\begin{aligned} &\|g_1(\alpha, t, N_1(t)) - g_1(\alpha, t, N_1^*(t))\| \\ &\quad = \|(-\rho + \alpha N_2(t) + \beta N_3)(N_1(t) \\ &\quad - N_1^*(t))\| \end{aligned}$$

Suppose that,

$$\xi_1 = \|(-\rho + \alpha N_2(t) + \beta N_3)\|$$

Once it is done, we can start writing.

$$\|g_1(\alpha, t, N_1(t)) - g_1(\alpha, t, N_1^*(t))\| \leq \xi_1(N_1(t) - N_1^*(t)) \quad (18)$$

$$\begin{cases} \|g_2(\alpha, t, N_2(t)) - g_2(\alpha, t, N_2^*(t))\| \leq \xi_2(N_2(t) - N_2^*(t)) \\ \|g_3(\alpha, t, N_3(t)) - g_3(\alpha, t, N_3^*(t))\| \leq \xi_3(N_3(t) - N_3^*(t)) \end{cases}$$

Where,

$\xi_2 = \|\mu\delta - (N_2(t) + N_2^*(t))\mu - \gamma N_1(t)\|$

$\xi_3 = \left\|\phi\eta - \left(N_3(t) + N_3^*(t)\right)\phi - \sigma N_1(t)\right\|$

As a result, we can see that the Lipschitz ideas worked. When the expressions in (18) are applied recursively, the following outcomes are obtained:

$$N_{1n}(t) - N_1(0) = \frac{1-v}{ABC(v)}\mathrm{g}_1\left(\alpha, t, N_{1n}(t)\right) + \frac{v}{ABC(v)\Gamma(v)}\int_0^t (t - \theta)^{v-1}\mathrm{g}_1\left(\alpha, t, N_{1n}(\theta)\right)d\theta$$

$$N_{2n}(t) - N_2(0) = \frac{1-v}{ABC(v)}\mathrm{g}_2\left(\alpha, t, N_{2n}(t)\right) + \frac{v}{ABC(v)\Gamma(v)}\int_0^t (t - \theta)^{v-1}\mathrm{g}_2\left(\alpha, t, N_{2n}(\theta)\right)d\theta$$

$$N_{3n}(t) - N_3(0) = \frac{1-v}{ABC(v)}\mathrm{g}_3\left(\alpha, t, N_{2n}(t)\right) + \frac{v}{ABC(v)\Gamma(v)}\int_0^t (t - \theta)^{v-1}\mathrm{g}_3\left(\alpha, t, N_{3n}(\theta)\right)d\theta$$

At this time, as

$N_{10}(t) = N_1(0), N_{20}(t) = N_2(0), N_{30}(t) = N_3(0)$

It is possible to build the following statement by making use of the contrasts that exist between sequential terms:

$$N_{1,n}(t) = N_{1n}(t) - N_{1n-1}(t) = \frac{1-v}{ABC(v)}\left(\mathrm{g}_1\left(v, t, N_{1n-1}(t)\right) - \mathrm{g}_1\left(\alpha, t, N_{1n-2}(t)\right)\right) + \frac{v}{ABC(v)\Gamma(v)}\int_0^t (t-\theta)^{v-1}\left(\mathrm{g}_1\left(\alpha, \eta, N_{1n-1}(\theta)\right) - \mathrm{g}_1\left(\alpha, \theta, N_{1n-2}(\theta)\right)\right)d\theta,$$

$$N_{2,n}(t) = N_{2n}(t) - N_{2n-1}(t) = \frac{1-v}{ABC(v)}\left(\mathrm{g}_2\left(\alpha, t, N_{2n-1}(t)\right) - \mathrm{g}_2\left(\alpha, t, N_{2n-2}(t)\right)\right) + \frac{v}{ABC(v)\Gamma(v)}\int_0^t (t-\theta)^{v-1}\left(\mathrm{g}_2\left(\alpha, \theta, N_{2n-1}(\theta)\right) - \mathrm{g}_2\left(\alpha, \theta, N_{2\,n-2}(\theta)\right)\right)d\theta,$$

$$N_{3,n}(t) = N_{3n}(t) - N_{3n-1}(t) = \frac{1-v}{ABC(v)}\left(\mathrm{g}_3\left(\alpha, t, N_{3n-1}(t)\right) - \mathrm{g}_3\left(\alpha, t, N_{3n-2}(t)\right)\right) + \frac{v}{ABC(v)\Gamma(v)}\int_0^t (t-\theta)^{v-1}\left(\mathrm{g}_3\left(\alpha, \theta, N_{3n-1}(\theta)\right) - \mathrm{g}_3\left(\alpha, \theta, N_{3n-2}(\theta)\right)\right)d\theta$$

Regarding this, it is crucial to remember that

$N_{1n}(t) = \sum_{i=0}^{n} N_{1_{N_{1,i}}}(t)$, $N_{2n}(t) = \sum_{i=0}^{n} N_{1_{N_{2,i}}}(t)$, $N_{3n}(t) = \sum_{i=0}^{n} N_{1_{N_{3,i}}}(t)$.

As an additional point of interest, in the setting of (18), which allows for

$N_{1_{N_{1,n-1}}}(t) = N_{1n-1}(t) - N_{1n-2}(t),$

$N_{1_{N_{2,n-1}}}(t) = N_{2n-1}(t) - N_{2n-2}(t),$

$N_{1_{N_{3,n-1}}}(t) = N_{3n-1}(t) - N_{3n-2}(t),$

It is possible to write.

$$\left\|N_{1_{N_{1,n}}}(t)\right\| \le \frac{v}{ABC(v)}\xi_1\left\|N_{1_{N_{1,n-1}}}(t)\right\| \frac{v}{ABC(v)\Gamma(v)}\xi_1\int_0^t (t-\theta)^{v-1}\left\|N_{1N_{1,n-1}}(\theta)\right\|d\theta,$$

$$\left\|N_{1_{N_{2,n}}}(t)\right\| \le \frac{v}{ABC(v)}\xi_1\left\|N_{1_{N_{2,n-1}}}(t)\right\| \frac{v}{ABC(v)\Gamma(v)}\xi_1\int_0^t (t-\theta)^{v-1}\left\|N_{1_{N_{2,n-1}}}(\theta)\right\|d\theta, \quad (19)$$

$$\left\|N_{1_{N_{3,n}}}(t)\right\| \le \frac{\alpha}{ABC(\alpha)}\xi_1\left\|N_{1_{N_{3,n-1}}}(t)\right\| \frac{v}{ABC(v)\Gamma(v)}\xi_1\int_0^t (t-\theta)^{v-1}\left\|N_{1_{N_{3,n-1}}}(\theta)\right\|d\theta,$$

Theorem 5: If the preceding condition is true for $t \in [0, p]$, then the fractional-order model (12) has a unique solution:

$\frac{1-v}{ABC(v)}\xi_i + \frac{v}{ABC(v)\Gamma(v)}p^v\xi_i < 1 \quad , \quad i = 1, 2, 3.$ (20)

Proof: It is a presumption that the functions $N_1(t), N_2(t), N_3(t)$ are all bounded. As a preliminary matter, equations (18) make it clear that $\mathrm{f}_1, \mathrm{f}_2, \mathrm{f}_3$ valid representations of the Lipschitz condition. Consequently, we get the following by using equation (21) together with a recursive hypothesis [34]:

$$\left\|N_{1_{N_{1,n}}}(t)\right\| \le \|N_{10}(t)\|\left(\frac{1-v}{ABC(v)}\xi_1 + \frac{vp^v}{ABC(v)\Gamma(v)}\xi_1\right)^n,$$

$$\left\|N_{1_{N_{2,n}}}(t)\right\| \le \|N_{20}(t)\|\left(\frac{1-v}{ABC(v)}\xi_2 + \frac{vp^v}{ABC(v)\Gamma(v)}\xi_2\right)^n, \quad (21)$$

$$\left\|N_{1_{N_{3,n}}}(t)\right\| \le \|N_{30}(t)\|\left(\frac{1-v}{ABC(v)}\xi_3 + \frac{vp^v}{ABC(v)\Gamma(v)}\xi_3\right)^n$$

As a result, when the value of n approaches$n \to \infty$, the sequences mentioned above are valid and hold$\left\|N_{1_{N_{1,n}}}(t)\right\| \to 0, \left\|N_{1_{N_{2,n}}}(t)\right\| \to 0, \left\|N_{1_{N_{3,n}}}(t)\right\| \to 0.$

Furthermore, employing the triangle inequality, equation (21) can be stated in the following manner:

$$\left\|N_{1_{N_{1n+m}}}(t) - N_{1_{N_{1n}}}(t)\right\| \leq \sum_{j=n+1}^{n+m} \Psi_1^j = \frac{\Psi_1^{n+1} - \Psi_1^{n+m+1}}{1-\Psi_1},$$

$$\left\|N_{1_{N_{2n+m}}}(t) - N_{1_{N_{2n}}}(t)\right\| \leq \sum_{j=n+1}^{n+m} \Psi_2^j = \frac{\Psi_2^{n+1} - \Psi_2^{n+m+1}}{1-\Psi_2},$$

$$\left\|N_{1_{N_{3n+m}}}(t) - N_{1_{N_{3n}}}(t)\right\| \leq \sum_{j=n+1}^{n+m} \Psi_3^j = \frac{\Psi_3^{n+1} - \Psi_3^{n+m+1}}{1-\Psi_3}, \quad (22)$$

Where, $\Psi_i = \frac{1-v}{ABC(v)}\xi_i + \frac{v}{ABC(v)\Gamma(v)}p^v\xi_i < 1$ by hypothesis.

Hyers-Ulam stability

Definition: Assuming the suggested model's ABC fractional-order integral form (12) is taken into consideration, Hyers-Ulam stability (Ullah and Kabir, 2024) is attained even if the values of $\forall\chi_i > 0$, $\exists$ constants $\omega_i > 0$, $i \in N^5$.

$$\left|N_1(t) - \frac{1-v}{ABC(v)}g_1(v,t,N_1(t)) + \frac{v}{ABC(v)\Gamma(v)}\int_0^t (t-\theta)^{v-1} g_1(v,\theta,N_1(\theta))\,d\theta\right| \leq \chi_1$$

$$\left|N_2(t) - \frac{1-v}{ABC(v)}g_2(v,t,N_2(t)) + \frac{v}{ABC(v)\Gamma(v)}\int_0^t (t-\theta)^{v-1} g_2(v,\theta,N_2(\theta))\,d\theta\right| \leq \chi_2 \quad (23)$$

$$\left|N_3(t) - \frac{1-v}{ABC(v)}g_3(v,t,N_3(t)) + \frac{v}{ABC(v)\Gamma(v)}\int_0^t (t-\theta)^{v-1} g_3(v,\theta,N_3(\theta))\,d\theta\right| \leq \chi_3$$

$\exists \left(\dot{N}_1(t), \dot{N}_2(t), \dot{N}_3(t)\right)$ which satisfying

$$\dot{N}_1(t) = \frac{1-v}{ABC(v)}g_1(t,N_1(t)) + \frac{v}{ABC(v)\Gamma(v)}\int_0^t (t-\theta)^{v-1} g_1\left(v,\theta,\dot{N}_1(\theta)\right)d\theta$$

$$\dot{N}_2(t) = \frac{1-v}{ABC(v)}g_2(t,N_2(t)) + \frac{v}{ABC(v)\Gamma(v)}\int_0^t (t-\theta)^{v-1} g_2\left(v,\theta,\dot{N}_2(\theta)\right)d\theta$$

$$\dot{N}_3(t) = \frac{1-v}{ABC(v)}g_3(t,N_3(t)) + \frac{v}{ABC(v)\Gamma(v)}\int_0^t (t-\theta)^{v-1} g_3\left(v,\theta,\dot{N}_3(\theta)\right)d\theta$$

Implies that

$$\left|N_1(t) - \dot{N}_1(t)\right| < \chi_1\xi_1\,, \left|N_2(t) - \dot{N}_2(t)\right| < \chi_2\xi_2, \left|N_3(t) - \dot{N}_3(t)\right| < \chi_3\xi_3 \quad (24)$$

Theorem 6: The given prey-predator fractional-order model (12) meets the Hyers-Ulam stability condition according to the ς criteria.

Proof: In accordance with Theorem 5, the fractional-order model (15) possesses a singular solution that is capable of fully satisfying the system of equation (16). Because of this, we are able to write (Ullah and Kabir, 2024),

$$\left|N_1(t) - \dot{N}_1(t)\right| \leq \frac{1-v}{ABC(v)}\left\|g_1(v,t,N_1(t)) - g_1\left(v,t,\dot{N}_1(t)\right)\right\| + \frac{v}{ABC(v)\Gamma(v)}\int_0^t (t-\theta)^{v-1}\left\|g_1(v,\theta,N_1(\theta)) - g_1\left(v,\theta,\dot{N}_1(\theta)\right)\right\|d\theta \leq \left[\frac{1-v}{ABC(v)} + \frac{v}{ABC(v)\Gamma(v)}\right]N_1\left\|N_1(t) - \dot{N}_1(t)\right\| \quad (25)$$

$$\left|N_2(t) - \dot{N}_2(t)\right| \leq \frac{1-v}{ABC(v)}\left\|g_2(v,t,N_2(t)) - g_2\left(\alpha,t,\dot{N}_2(t)\right)\right\| + \frac{v}{ABC(v)\Gamma(v)}\int_0^t (t-\theta)^{v-1}\left\|g_2(\alpha,\theta,N_2(\theta)) - g_2\left(\alpha,\theta,\dot{N}_2(\theta)\right)\right\|d\theta \leq \left[\frac{1-v}{ABC(v)} + \frac{v}{ABC(v)\Gamma(v)}\right]N_2\left\|N_2(t) - \dot{N}_2(t)\right\| \quad (26)$$

$$\left|N_3(t) - \dot{N}_3(t)\right| \leq \frac{1-v}{ABC(v)}\left\|g_3(v,t,N_3(t)) - g_3\left(v,t,\dot{N}_3(t)\right)\right\| + \frac{v}{ABC(v)\Gamma(v)}\int_0^t (t-\theta)^{v-1}\left\|g_3(v,\theta,N_3(\theta)) - g_3\left(v,\theta,\dot{N}_3(\theta)\right)\right\|d\theta \leq \left[\frac{1-\alpha}{ABC(\alpha)} + \frac{\alpha}{ABC(\alpha)\Gamma(\alpha)}\right]N_3\left\|N_3(t) - \dot{N}_3(t)\right\| \quad (27)$$

$$N_i = \chi_i, \frac{1-v}{ABC(v)} + \frac{v}{ABC(v)\Gamma(v)} = \theta_i.$$

Then we have

$$\|N_1(t) - \dot{N}_1(t)\| \leq \chi_1\theta_1 .$$
$$\|N_2(t) - \dot{N}_2(t)\| \leq \chi_2\theta_2 \quad (28)$$
$$\|N_3(t) - \dot{N}_3(t)\| \leq \chi_3\theta_3$$

One can determine the model's Hyers-Ulam stability (16) by examining equation (28). This proves the theorem correct by showing that the ABC fractional-order model (15) is Hyers-Ulam stable.

As observed in Fig. 9, showing the evolution of the student population for various values of ν (1.0, 0.9, 0.8, and 0.7), memory effects and non-integer differentiation influence system stability. This line underlines the significance of fractional-order modeling in educational dynamics by illustrating how transient behavior changes as ν drops, therefore producing different equilibrium states and convergence rates.

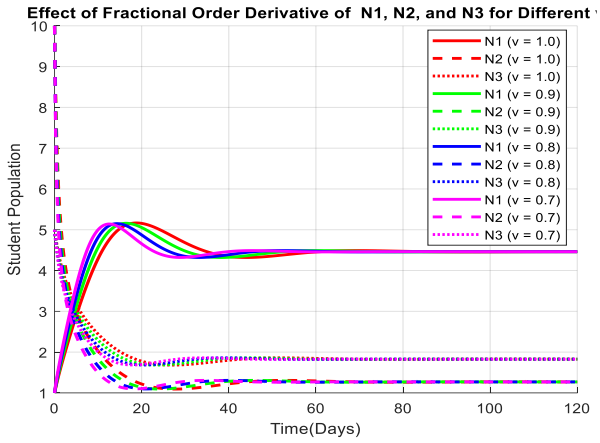

Fig. 9. Effect of the fractional-order derivative ν on the dynamics of academic pressure (N_1), undergraduate students (N_2), and graduate students (N_3) over time using the model (12).

Fig. 10 demonstrates how the oscillatory behavior and stability of N_1 are changed by varying ν from 1.0
to 0. 7. The fact that the persistence of oscillations is strengthened with decreasing ν values indicates the effect of memories and fractional interactions on the fluctuating and steady-state behavior of the system.

Fig. 11 indicates that, despite prolonged shifts occurring with lower ν, the undergraduate student population recovers more quickly with larger ν, implying that the effects of academic pressure last for a longer period of time, The fractional-order method accounts for long-term memory to better capture real student behavior.

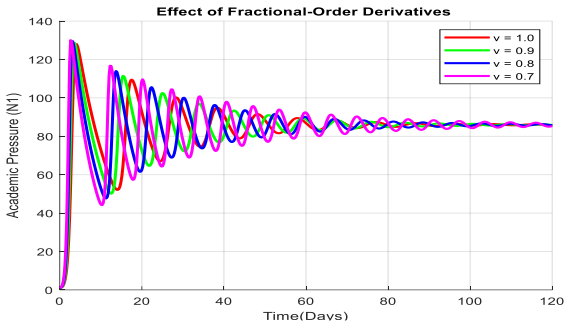

Fig. 10. Effect of fractional-order derivatives (ν) on academic pressure (N_1) over time using the model (12).

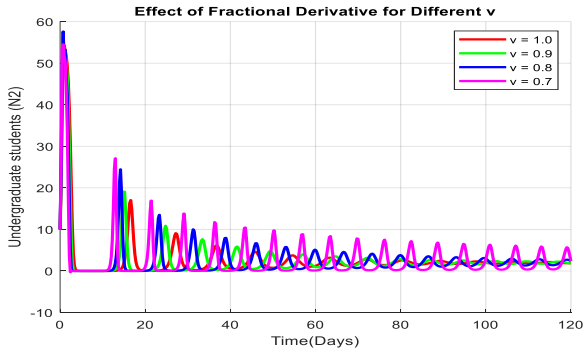

Fig. 11. Effect of fractional-order derivatives (v) on undergraduate students (N_2) over time using the model (12).

Fig.12 shows that convergence accelerates as v increases, implying that graduate students rapidly adapt to higher levels of academic pressure. Conversely, lower v causes changes to persist longer, implying that the system is unstable for a longer period since memory effects are stronger. These memory-driven responses better capture graduate students' behavior in shifting intellectual environments.

Numerical simulation with academic dynamics of the deterministic approach

A simulation of academic pressure (N_1) that affects

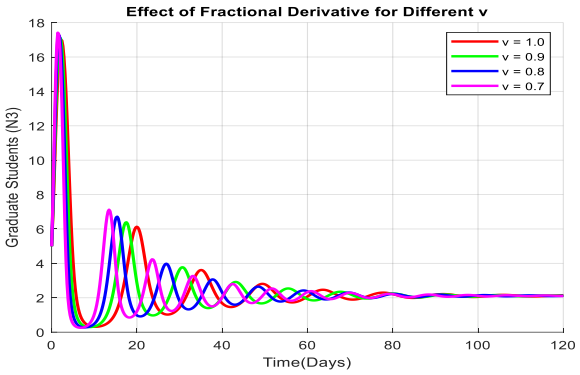

Fig. 12. Effect of fractional-order derivatives (v) on graduate students (N_3) over time using the model (12).

undergraduate students $(N_2)$and graduate students (N_3) are studied via the predator-prey model. This model demonstrates how population oscillations are influenced by stress levels, resilience, and external support systems in the academia.

High levels of academic stress lead to a sharp decline in the undergraduate student population,as shown in Fig. 1. Reflecting trends across academic stress levels, graduate students, and undergraduates react slowly. One gets a continuous

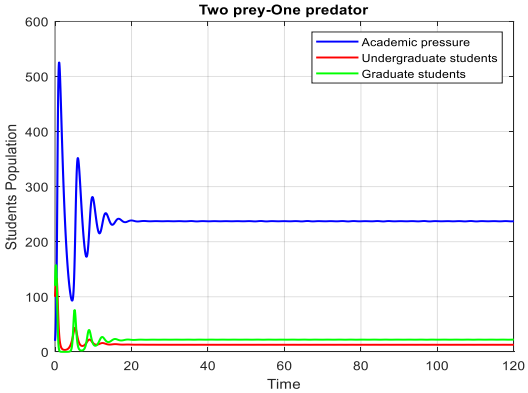

Fig. 13. Dynamical behavior of prey-predator model (1); Assume

$$\rho = 0.7, \alpha = 0.02, \beta = 0.02, \mu = 0.01,$$
$$\delta = 250, \gamma = 0.01, \lambda = 0.04,$$
$$\eta = 200, \sigma = 0.03.$$

equilibrium whereby stress and student populations coexist when the oscillations in all three populations are lowered over time. Students who act in this way areobviously gradually adjusting to school life ands are able to control their tension. As shown in Fig. 13(a), the phase space trajectory converges to a single stable equilibrium point after spiralling inward.

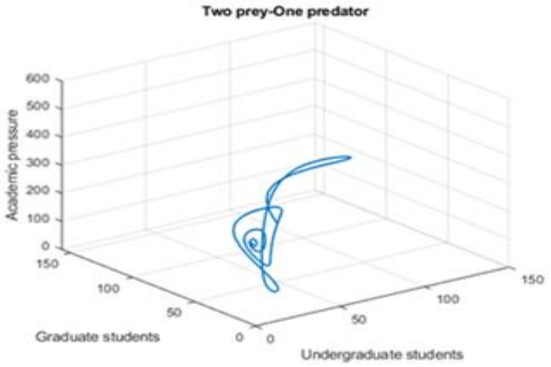

Fig. 13(a). Phase portrait.

Based on Fig. 14, damping in this system is smaller than in Fig. 13; oscillations last more before stabilizing. While undergraduate and graduate students show coincidence, the

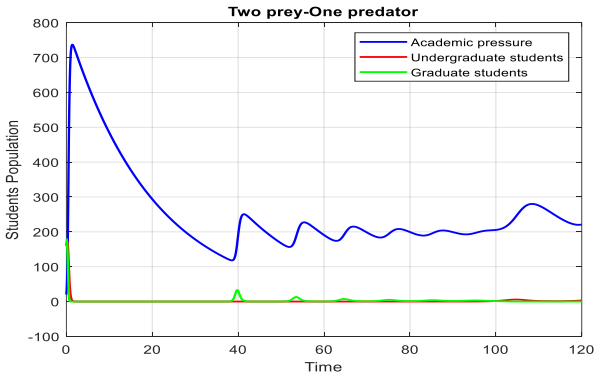

Fig. 14. Dynamical behavior of prey-predator model (1); Assume.

$$\rho = 0.7, \alpha = 0.02, \beta = 0.02, \mu = 0.01,$$
$$\delta = 250, \gamma = 0.01, \lambda = 0.04,$$
$$\eta = 200, \sigma = 0.03.$$

oscillations in stress populations exhibit different amplitudes over time. Under these conditions, the system is more sensitive, and periodic shocks delay stability

through recovery processes. Switching now to Fig. 14(a), the phase-space path forms a spiral that steadily appreoaches the equilibrium point.

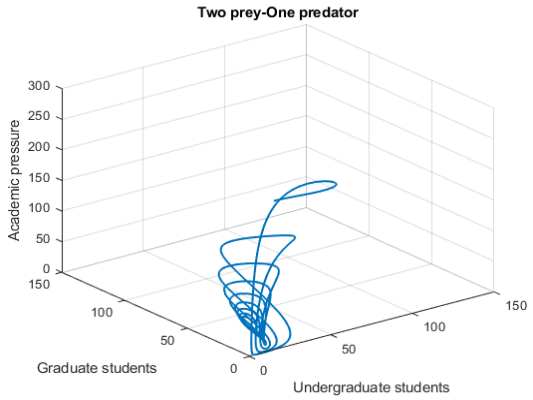

Fig. 14(a). Phase portrait.

As Fig. 15 shows, unlike the systems shown in Figs. 13 and 14, this one lacks damping. For academic stress among undergraduate and graduate students, the data show constant-amplitude, continuous oscillations. We argue that the system is in a limit cycle as these oscillations continue; it is dynamic but has not attained equilibrium. Here,

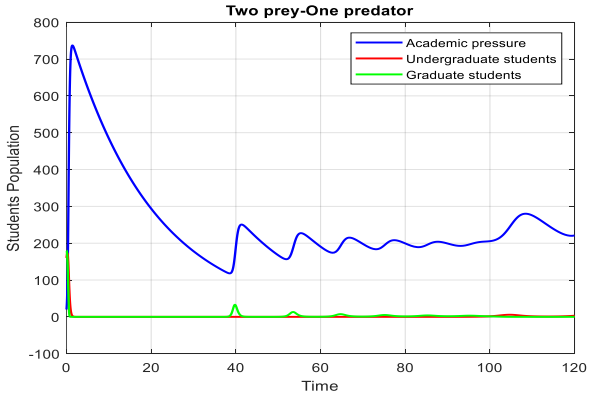

Fig. 15. Dynamical behavior of prey-predator model (1); Assume

$\rho = 0.05, \alpha = 0.02, \beta = 0.02, \mu = 0.01,$
$\delta = 250, \gamma = 0.01, \lambda = 0.04,$
$\eta = 200, \sigma = 0.03$

cyclical stressors, including semester scheduling and external factors, make academic ecosystem stability unreachable. Limit cycle dynamics are suggested by the closed loop in the phase diagram depicted in Fig. 15(a). This defines the lack of equilibrium and the existence of ongoing oscillatory action.

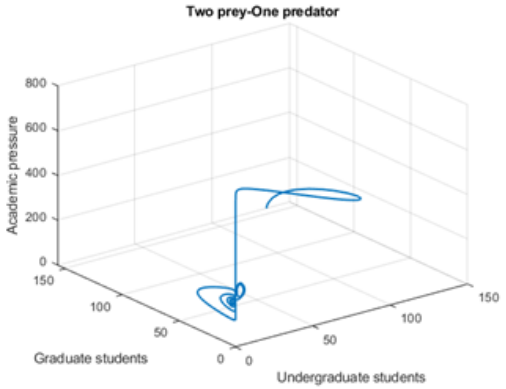

Fig.15(a). Phase portrait.

The system shows continuous oscillations in Fig. 16, consistent with Fig. 15 but with higher amplitudes. These indicators point to more intense interactions among individuals, which cause more stress and changes the student body. The system maintains a dynamic, oscillatory condition with substantial time-span fluctuations. Although the phase plot still

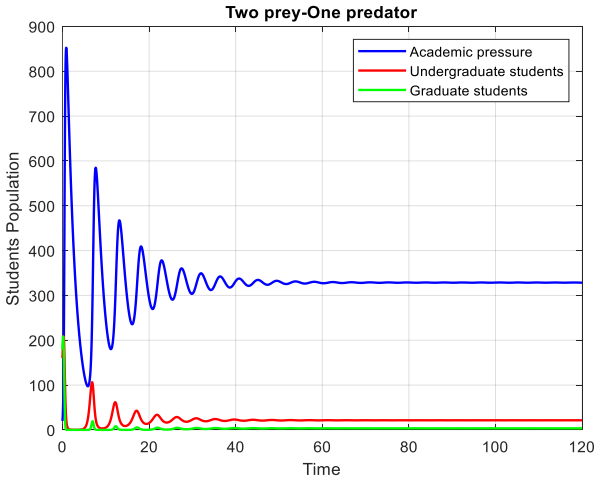

Fig. 16. Dynamical behavior of prey-predator model (1); Assume

$\rho = 0.5, \alpha = 0.02, \beta = 0.02, \mu = 0.01, \delta = 350, \gamma = 0.01, \lambda = 0.04,$
$\eta = 250, \sigma = 0.03$

shows complete loops, the trajectories in Fig. 16(a) span a greater region than in Fig. 16(a), implying bigger oscillation amplitudes. The interaction among

academic pressure, undergraduates, and graduates appears more complex and dynamic.

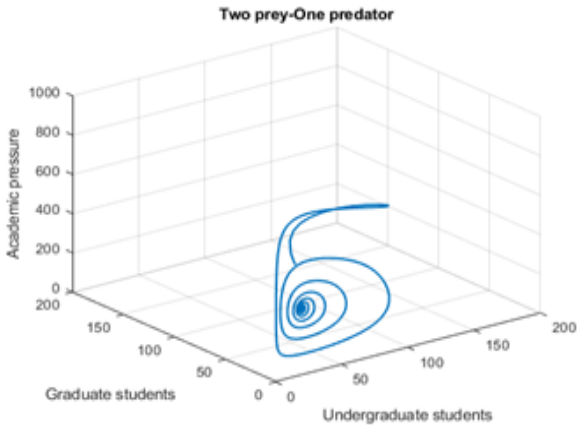

Fig. 16(a). Phase portrait.

Lyapunov exponent

Finding the Lyapunov exponent, a gauge of the system's sensitivity to its initial conditions, helps determine whether a system is periodic, chaotic, or stable. The red curve indicates the proportion of pupils influenced by academic pressure; mostly undergraduate students make up this group. Because graduate students can control or stabilize system dynamics, academic pressure subtly targets them.

From Fig. 17(a), at $\alpha = 0.82$, academic pressure (blue) shows significant disorder in its early stage, indicating a predator vulnerable to prey population shifts. The system responds to stress and finally resolves this state. First, undergraduates' chaotic dynamics indicate significant sensitivity to academic pressure. Graduate students faced more challenges due to resource scarcity and academic pressure. By maintaining stability, graduatestudents (green) prevent system collapse. Undergraduate academic obligations can be onerous and unstable. Maintaining fair academic standards to prevent academic stress among graduating students benefits the overall educational system.

From Fig. 17(b) for $\alpha = 0.2$, academic pressure (blue) has a shorter chaotic phase than (a), indicating stronger predator efficiency due to faster response to prey population changes. Academic pressure is a predator; therefore, undergraduates are less chaotic at first, yet still fluctuate. Graduate student competition decreases as the system stabilises. Graduate students (green) aren't afraid of predators or rivals like undergraduates. Effective academic pressure stabilises predators faster. Graduate students pose fewer hazards, but undergraduates are becoming stable.

From Fig. 17(c), the predator responds well to system changes, leading to predictable, controllable stress levels. Academic Pressure (Blue) stabilises at $\alpha = 0.3$, exhibiting little chaos. Academic pressure reduces early turmoil and stabilises red undergraduates, making their population more predator-resistant. Graduate students (Green) are less volatile under academic pressure or competition than undergraduates. Academic pressure on prey populations is decreasing, bringing the system closer to balance. Undergraduates can see that stress management works since graduate students are more stable.

From Fig. 17(d), academic pressure (blue) shows no chaotic phase and rapid stabilisation at $\alpha = 0.6$, indicating well-regulated behaviour and no longer causing instability in predator behaviour. The undergraduate population (red) establishes equilibrium early, reducing stress. Different from undergraduates, graduate students (green) are stable and unaffected by predators or competitors. Academic pressure is so strong, persistent, and long-lasting that the two prey populations may coexist. Graduate students give stability, whereas undergraduates are adaptable in ideal circumstances.

Low α causes the undergraduate population to become unstable and chaotic, while high α decreases chaos, speeds up stabilization, and maintains a balance between academic pressure and student populations.

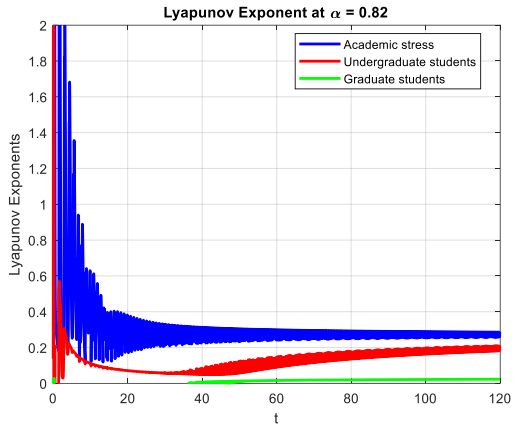

(a) Lyapunov exponent analysis $\alpha = 0.82$.

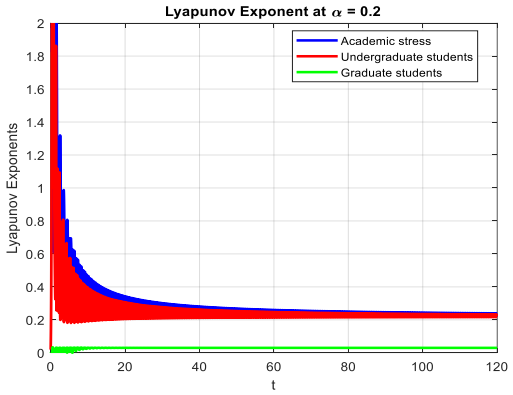

(b) Lyapunov exponent analysis $\alpha = 0.6$.

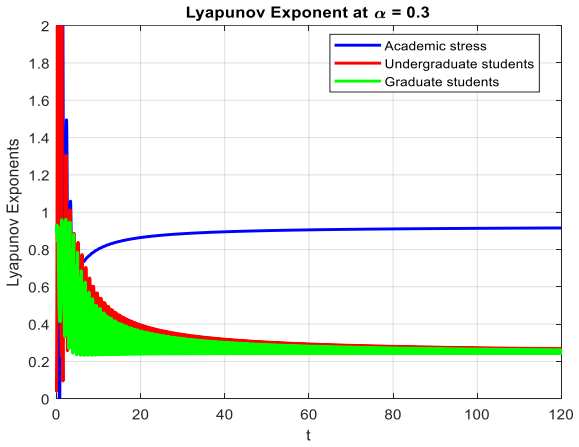

(**c) Lyapunov exponent analysis** $\alpha = 0.3$.

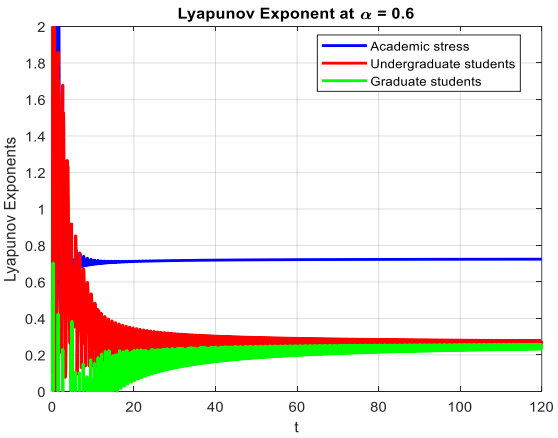

(d) Lyapunov exponent analysis $\alpha = 0.6$.

Fig. 17. System dynamics under varying academic pressure efficiency (α) using Lyapunov exponent analysis, highlighting the interactions between academic pressure (blue), undergraduate students (red), and graduate students (green) using the model (1).

Bifurcation diagrams of the model (1) under varying parameter values

Bifurcation diagrams of model (1) indicate significant thresholds at which qualitative alterations in system dynamics occur under different parameter values. These thresholds show variations between oscillatory and steady behavior.

As shown in Fig. 18(a-d), the breakdown of order from periodic stability is evidence of how increasing levels of external stress or strain disturb the delicate equilibrium between student populations and academic commitments. Students subjected to the anarchic system face uncertain academic demands, which could result in low marks, higher student dropout rates, and mental health difficulties. When ρ is small, small adjustments may be enough to stabilize the system and lessen oscillations. Stabilizing the chaotic dynamics at high value ρ requires systemic change, including lowering the workload.

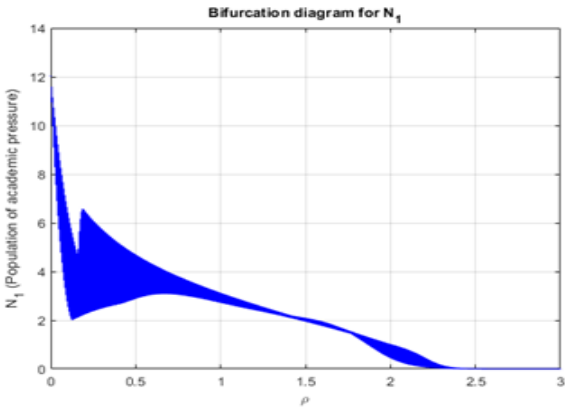

(a) **Bifurcation for** $\rho = 1900.$

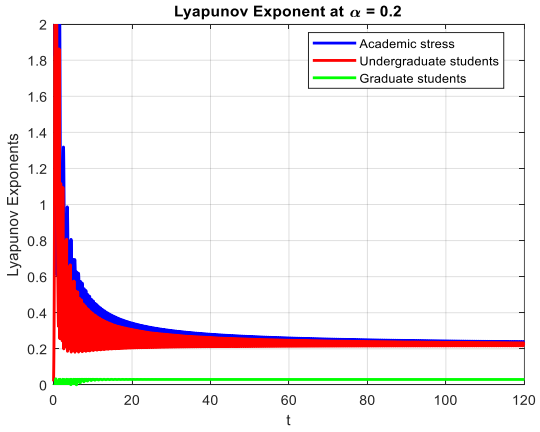

(b) Bifurcation for $\rho = 2800.$

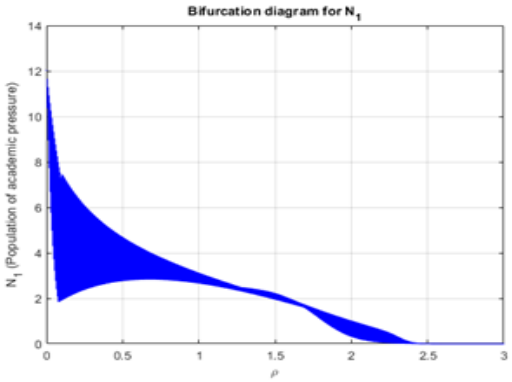

(c) Bifurcation for $\rho = 2900.$

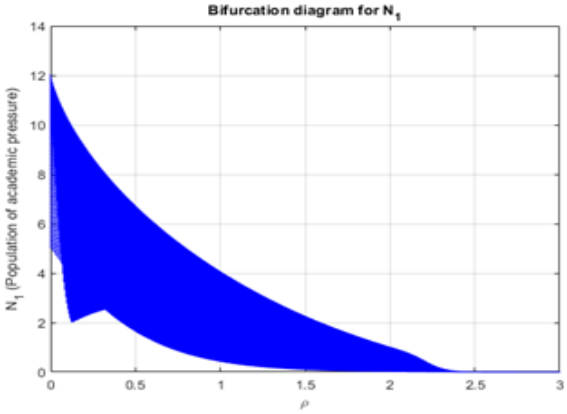

(d) Bifurcation for $\rho = 3800.$

Fig. 18. Bifurcation diagrams of academic pressure (N_1) under varying parameter values, showing chaotic behavior for: (a) $\rho = 1900,$ **(b)** $\rho = 2800,$ **(c)** $\rho = 2900,$ **and (d)** $\rho = 3800.$

As shown in Fig. 19(a-d) demonstrate how, as μ grows, the behavior transitions from stable to chaotic.

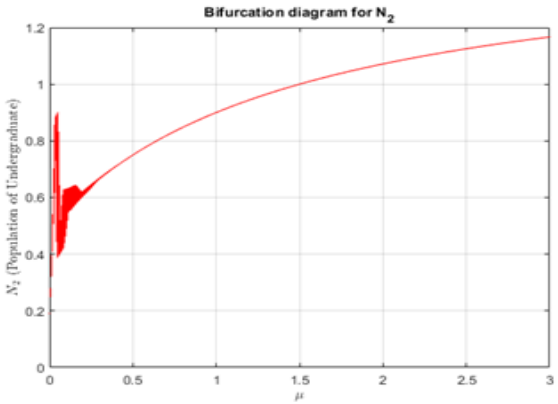

(a) Bifurcation for $\mu = 0.01.$

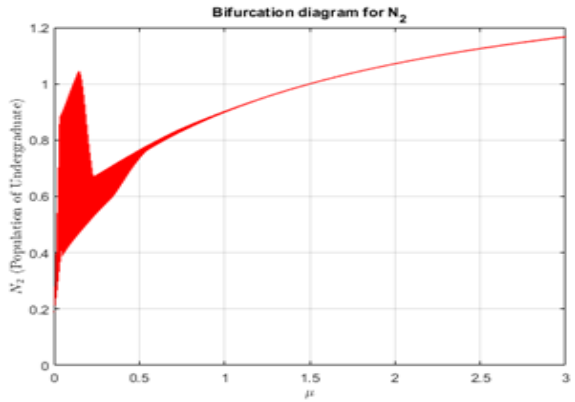

(b) Bifurcation for $\mu = 1.$

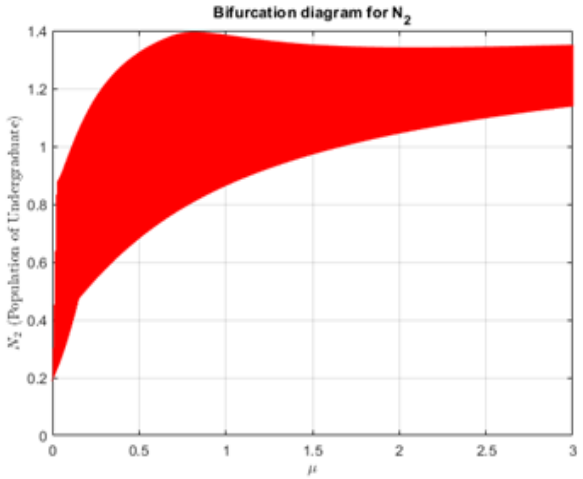

(c) Bifurcation for $\mu = 0.02$.

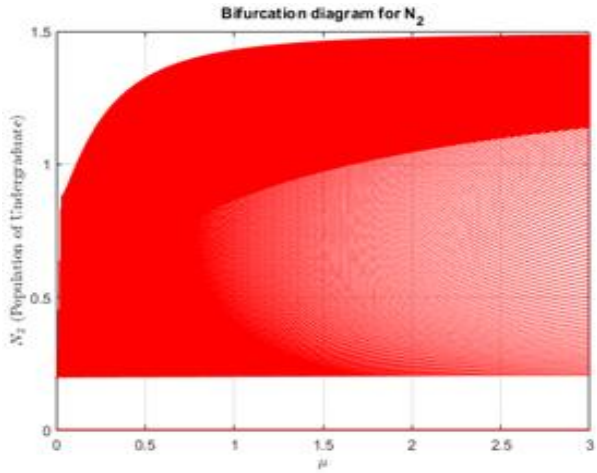

(d) Bifurcation for $\mu = 0.03$.

Fig. 19. Bifurcation diagrams of undergraduate students N_2 under varying parameter values, showing chaotic behaviour for: (a) $\mu = 0.01$, (b) $\mu = 1$, (c) $\mu = 0.02$, and (d) $\mu = 0.03$.

Changes to the starting points, parameter values, and model structure may cause the graphs to diverge, as indicated by the inconsistencies. The question of whether the system's stability is due to control mechanisms and critical thresholds arises when orderly regions are found within otherwise chaotic regions.

Basin of attraction

The depicted basin of attraction in the fractional-order predator-prey system comprising academic stress (N_1), undergraduate students (N_2) shows the areas of initial conditions that lead to a specific long-term behavior. The basin's grid-like form indicates it is most certainly a multi-attractor complicated dynamical system.

Fig. 20 shows a high academic-stress state (red region) across virtually all initial conditions of academic pressure (N_1) and undergraduate population (N_2), as indicated by the basin-of-attraction plot. The system is susceptible to the starting point of academic stress, as there is only a small area (blue region) near extremely low initial academic stress levels that leads to a low-stress equilibrium. This indicates that academic pressure is the primary factorinfluencingthe system's behaviorover the long run, and that resilience is low when stress levels are high.

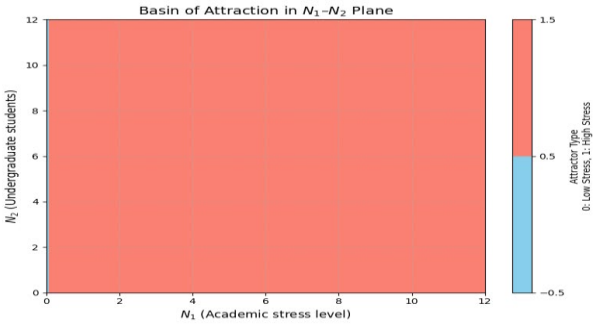

Fig. 20. Basin of attraction for the predator-prey dynamics among the academic stress (N_1) and undergraduate students (N_2) using the model (1).

Sensitivity analysis

Sensitivity analysis is one mathematical tool that helps one understand how modifying model parameters affects system output. In ecological, social, and biological models, sensitivity analysis is especially helpful for identifying which factors most affect the behavior of dynamic systems. To evaluate the influence of parameter x_i on the basic reproduction number(R_0), the corresponding sensitivity index is determined as follows:

$$\tau_{x_i}^{R_0} = \frac{\partial R_0}{\partial x_i} \times \frac{x_i}{R_0} \tag{29}$$

This tells us the relative change in R_0 resulting from a relative change in ρ. Let's derive and interpret each sensitivity analytically:

Using Eq. (29) and the parameter values provided in Table 2, the sensitivity indices of the basic reproduction number R_0 are evaluated and presented in Table 5.

Table 5. Sensitivity analysis.

Parameter	Sensitivity index $(\tau_{x_i}^{R_0})$	Interpretation
α	$\tau_{\alpha}^{R_0} = \frac{\alpha\delta}{\alpha\delta+\beta\eta} = 0.25$	Positive
β	$\tau_{\beta}^{R_0} = \frac{\beta\eta}{\alpha\delta+\beta\eta} = 0.75$	Positive
δ	$\tau_{\delta}^{R_0} = \frac{\alpha\delta}{\alpha\delta+\beta\eta} = 0.25$	Positive
η	$\tau_{\eta}^{R_0} = \frac{\beta\eta}{\alpha\delta+\beta\eta} = 0.75$	Positive
ρ	$\tau_{\rho}^{R_0} = \frac{\alpha\delta+\beta\eta}{\rho^2}.\frac{\rho}{R_0} = -1$	Negative

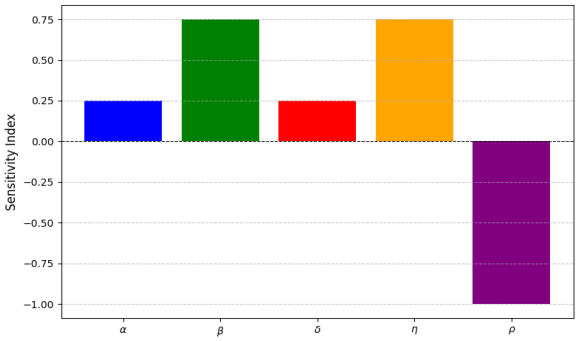

Fig. 21. Normalized sensitivity indices of the basic reproduction number $(R_0)$with respect to model parameters.

As shown in Table 5 and Fig. 21, the most sensitive parameters of the basic reproduction number $(R_0)$are β and η, both having a positive sensitivity index of 0.75. Here, β represents the degree to which academic pressure affects graduate students, while η denotes the environment's carrying capacity for graduate students. This means that a 1% increase in either parameter leads to a 0.75% increase in R_0. The parameters α and δ, which indicate the efficiency of academic pressure affecting undergraduate students and carrying capacity for undergraduate students, respectively, each have a lower but still positive sensitivity index of 0.25. On the other hand, ρhas a negative sensitivity index of –1, implying that a 1% increase in ρ results in a 1% decrease in R_0.

Conclusion

The fractional-order predator-prey model is effective for depicting the dynamics of students' academic stress. Stability analysis and bifurcation theory demonstrate how various stress levels allow students to experience stable, oscillatory, and unstable states. The equilibrium point becomes unstable and frequent limit cycles start as the eigenvalues have crossed zero when the value of ρ approaches 1.2. The system exhibits oscillatory behavior at this threshold ($\rho > 1.2$), so excessive academic stress might cause instability in student Performance (Fig. 4). Variations in the bifurcation parameter ρ affect academic stress, with a Neimark-Sacker bifurcation at ρ around 1.4 and oscillatory instability emerging as α increases beyond 1.2–1.5. Quasiperiodic behaviour starts near α approximately 1.3, leading to instability when eigenvalues cross the unit circle. It identifies a clear point of global asymptotic stability by applying the predator-prey model to capturing academic pressure among undergraduate and graduate students in a higher education institution. Looking at the phase profiles and Lyapunov function in Fig. 8, all trajectories converge to the same special equilibrium point independent of the initial conditions.

Specifically, we argue that when stress responses exhibit lag effects or long-term memory, such as recurring academic anxiety, the fractional approach captures these effects more clearly as shown in Figs. 9, 10, 11, and 12. While higher values of ν enable faster convergence, lower values lead to sustained oscillations. Both academic stress and student populations exhibit oscillatory patterns; the former shows a stable equilibrium, while the latter shows continuous limit cycles of varying amplitudes. Increased academic pressure (N_1) may be the reason for lower enrollment in undergraduate programs (N_2)

, as students either terminate or do not finish their degrees. According to Fig. 13, academic pressure ranges from 550 to 600 before settling at 250 to 300 for students. Fig. 13(a) with its phase-space analysis reveals dynamic pressure-student interactions. With oscillation periods ranging from about 10 to 20 time units, initial peaks of 310, 150, and 130 for N_1, N_2, and N_3 as shown in Fig. 14, point to a predator-prey link. Fig. 14(a) exhibits a spiralling contraction stabilizing around (50, 30, and 30) in 100 time units. Whereas the 3D phase portrait in Fig. 15(a) shows a spiral contraction towards stability, achieving equilibrium within 100–120 time units, academic pressure peaks at 700 in Figure 10 and then falls suddenly. Fig. 16 shows academic pressure beginning at 800 and stabilizing at about 300. The population of both undergraduate and graduate students falls to almost zero. The 3D phase space in Fig. 16(a) shows a spiral trajectory, suggesting that academic pressure preys on students, leading to a stable state with low student populations. When ρ is low, academic pressure is quite erratic and variable; this could be the result of outside factors. The stabilization of pressure levels as ρ increases suggests that specific guidelines or policies could help control the ups and downs of academic strain. As shown in Fig. 21, β and η significantly increase R_0, while α and δ moderately increase it; ρ strongly decreases it.

The ordinary differential equation (ODE) model is appropriate for scenarios where the response to academic stress is assumed to be immediate or lacks memory. The fractional-order model, particularly using the ABC derivative, is better suited for real-world educational systems, where the impact of academic stress is persistent and cumulative over time. This implies that, apart from this quality, other elements influence academic stress more strongly. Based on a thorough mathematical model impact analysis, our future plan aims to reduce student stress, improve academic performance, and enhance general well-being by creating a more favorable and efficient educational environment through adaptive control parameters.

Acknowledgment

The authors sincerely thank all individuals who provided valuable suggestions, insightful discussions, and constructive feedback that significantly contributed to the improvement and successful completion of this research work.

Authors contribution

Md. Asraful Islam conceived and designed the study, formulated the deterministic and fractional-order mathematical model, performed the analytical derivations and theoretical proofs, conducted stability, persistence, and bifurcation analyses, executed numerical simulations, interpreted the results, and prepared the original manuscript draft. Tanvir Ahmed contributed to the literature review, assisted with the review of analytical results, supported manuscript editing and formatting, and provided critical revisions. Both authors read and approved the final version of the manuscript.

Conflict of interest

The authors declare that there is no conflict of interest regarding the publication of this paper.

Reference

Ahmed N, Yasin MW, Akgül A, Baleanu D and Mircea OT. Mathematical analysis and pattern formation in diffusive predator–prey system. *J. Appl. Math.Comput.* 2025; 15(1): 580-622.

Amri A, Khan KAN and Qamar JA. Combining impact of velocity, fear and refuge for the predator–prey dynamics. *J. Biol. Dyn.* 2023; 17(1): 2181989.

Bai D, Li J and Zeng W. Global stability of the boundary solution of a nonautonomous predator–prey system with Beddington–DeAngelis functional response. *J. Biol. Dyn.* 2020; 14(1): 421-437.

Bai L, Li J, Zhang K and Zhao W. Analysis of a stochastic ratio-dependent predator–prey model driven by Lévy noise. *Appl. Math. Comput.* 2014; 233: 480-493.

Bai Y and Li Y. Stability and hopf bifurcation for a stage-structured predator–prey model incorporating refuge for prey and additional food for predator. *Adv. Differ. Equ.* 2019; 2019: 42.

Christle CA, Jolivette K and Nelson CM. School characteristics related to high school dropout rate. *Rem. Spec. Educ.* 2007; 28(6): 325-339.

Deng H, Chen F, Zhu Z and Li Z. Dynamic behaviors of Lotka–Volterra predator–prey model incorporating predator cannibalism. *Adv. Differ. Equ.* 2019; 2019(1): 359.

Dubey B, Kumar A andMaiti AP. Global stability and Hopf bifurcation of a prey–predator system with two discrete delays, including habitat complexity and prey refuge. *Commun. Nonlinear Sci. Numer. Simula.*, 2019; 67: 528-554.

Gokila C, Sambath M, Balachandran K and MaYK. Stationary distribution and global stability of a stochastic predator–prey model with disease in the prey population. *J. Biol. Dyn.* 2023; 17(1): 2164803.

Hone ANW, Irle MD and Thurura GW. On the neimark–sacker bifurcation in a discrete predator–prey system. *J. Biol. Dyn.* 2010; 4(6): 594-606.

Hu D and Cao H. Stability and bifurcation analysis in a predator–prey system with michaelis–mententype predator harvesting. *Nonlinear Anal. Real World Appl.* 2017; 33: 58-82.

Islam MA and Ahmed T. Modeling and stability analysis of the dynamics of prey–predator population. *Jagannath Univ. J. Sci*.2024; 11(1): 81-93.

Islam MA, Hassan IR and Ahmed P. Dynamic complexity of fifth-dimensional Henon map with Lyapunov exponent, permutation entropy, bifurcation patterns, and chaos. *J. Comput. Appl. Math.* 2025; 466: 116547.

Jiang G, Lu Q and Qian L. Complex dynamics of a Holling type II prey–predator system with state feedback control. *Chaos Solition Fract.* 2007; 31(2): 448-461.

Li F and Li H. Hopf bifurcation of a predator–prey model with time delay and stage structure for the prey. *Math.Comput. Model.* 2012; 55(3-4): 672-679.

Liu M, He X and Yu J. Dynamics of a stochastic regime-switching predator–prey model with harvesting and distributed delays. *Nonlinear Anal. Hybr. Syst.* 2018; 28: 87-104.

Lotka AJ. *Elements of Physics Biolology*.1st ed., *Williams & Wilkins Co., Baltimore*. 1925;pp. 1-495.

Ma Z, Li W, Zhao Y, Wang W, Zhang H and Li Z. Effects of prey refuges on a predator–prey model with a class of functional responses: The role of refuges. *Math. Bio. Sci.* 2009a; 218(2): 73-79.

Ma ZP, Huo HF and Liu CY. Stability and Hopf bifurcation analysis on a predator–prey model with discrete and distributed delays. *Nonlinear Anal. Real World Appl.* 2009b; 10(2): 1160-1172.

Misra AK and Dubey B. A ratio-dependent predator–prey model with delay and harvesting. *J. Biol. Syst.* 2010; 18(2): 437-453.

Mondal B, Roy S, Ghosh U and Tiwari PK. A systematic study of autonomous and nonautonomous predator–prey models for the combined effects of fear, refuge, cooperation, and harvesting. *Europ. Phys. J. Plus*, 2022; 137: 724.

Respondek L, Seufert T,StupniskyR and NettUE. Perceived academic control and academic emotions predict undergraduate university student success: Examining effects on dropout intention and achievement. *Front. Psychol.* 2017; 8, 243.

Sha A, Samanta S, Martcheva M and Chattopadhyay J. Backward bifurcation, oscillations, and chaos in an eco-epidemiological model with fear effect. *J. Biol. Dyn.* 2019;13(1): 301-327.

Ska N, Tiwari PK, Pal S andMartcheva M. A delay non-autonomous model for the combined effects

of fear, prey refuge, and additional food for predator. *J. Biol. Dyn.* 2021; 15(1): 580-622.

Song X, Hao M and Meng X. A stage-structured predator–prey model with disturbing pulse and time delays. *Appl. Math. Model.* 2009; 33(1): 211-223.

Tuerxun N, Abdurahman X and Teng Z. Global dynamics and optimal harvesting in a stochastic two-predators one-prey system with distributed delays and Lévy noise. *J. Biol. Dyn.*, 2020; 14(1): 32-56.

Ullah MS and Kabir KMA. Behavioral game of quarantine during the monkeypox epidemic: Analysis of deterministic and fractional order approach. *Heliyon*, 2024; 10(5):e26998.

Wang C and Yang W. Impact of nonlocal fear effect and mutual interference between predators in a diffusive predator–prey model. *J. Appl. Math. Comput.* 2025;69: 2155-2176.

Wang W, Zhu Y, Cai Y and Wang W. Dynamical complexity induced by Allee effect in a predator–prey model. *Nonlinear Anal. Real World Appl.* 2014; 16: 103-119.

Wei F and Fu Q. Hopf bifurcation and stability for predator–prey systems with Beddington–DeAngelis type functional response and stage structure for prey incorporating refuge. *Appl. Math. Model.* 2016; 40(1): 126134.

Xiang C, Huang J and Wang H. Bifurcations in Holling-Tanner model with generalist predator and prey refuge. *J. Differ. Equ.* 2023; 343: 495-529.

Yu T, Tian Y and Guo SH. Dynamical analysis of an integrated pest management predator–prey model with weak Allee effect. *J. Biol. Dyn.* 2019; 13(1): 218-244.

Zheng J, Wang Z, Li Y and Wang J. Bifurcations and chaos in a three-dimensional generalized Hénon map. *Adv. Differ. Equ.* 2018; 2018(1): 185.

Zhu X, Wang H and Ouyang Z. The state-dependent impulsive control for a general predator–prey model. *J. Biol. Dyn.*, 2022; 16(1): 354-372.